ARTICLE

Two target gene activation pathways for orphan ERR nuclear receptors

Tomoyoshi Nakadai[1,2], Miho Shimada[1,3], Keiichi Ito[1], Murat Alper Cevher[1,4], Chi-Shuen Chu[1], Kohei Kumegawa[5], Reo Maruyama[2], Sohail Malik[1] and Robert G Roeder[1]✉

Estrogen-related receptors (ERRα/β/γ) are orphan nuclear receptors that function in energy-demanding physiological processes, as well as in development and stem cell maintenance, but mechanisms underlying target gene activation by ERRs are largely unknown. Here, reconstituted biochemical assays that manifest ERR-dependent transcription have revealed two complementary mechanisms. On DNA templates, ERRs activate transcription with just the normal complement of general initiation factors through an interaction of the ERR DNA-binding domain with the p52 subunit of initiation factor TFIIH. On chromatin templates, activation by ERRs is dependent on AF2 domain interactions with the cell-specific coactivator PGC-1α, which in turn recruits the ubiquitous p300 and MED1/Mediator coactivators. This role of PGC-1α may also be fulfilled by other AF2-interacting coactivators like NCOA3, which is shown to recruit Mediator selectively to ERRβ and ERRγ. Importantly, combined genetic and RNA-seq analyses establish that both the TFIIH and the AF2 interaction-dependent pathways are essential for ERRβ/γ-selective gene expression and pluripotency maintenance in embryonic stem cells in which NCOA3 is a critical coactivator.

Cell Research (2023) 33:165–183; https://doi.org/10.1038/s41422-022-00774-z

INTRODUCTION

Control of transcription by RNA polymerase II (Pol II) involves regulated formation of multiprotein complexes at the promoter and enhancer regions of the target genes. These complexes are primarily nucleated by site-specific DNA-binding transcription factors (activators and repressors) that respond to cellular, developmental and environmental signals.[1] Transcriptional activators, including members of the large nuclear receptor (NR) superfamily, recruit a series of coactivators that serve both to overcome the chromatin barrier and to directly facilitate the entry of Pol II and its associated general transcription factors (GTFs) to generate the transcriptionally active preinitiation complex (PIC).[1] Coactivators acting at the level of chromatin[2] include both the ATP-dependent chromatin remodeling factors and enzymes that generate covalent modifications of specific residues in nucleosomal histones. Among the histone-modifying enzymes, p300 is particularly well studied and acetylates histone H3, which both decompacts chromatin and leads to recruitment of acetyl-lysine-binding effector proteins.[3] The other major class of coactivators is represented by the TAF components of TFIID[4] and by Mediator, a multiprotein complex that directly regulates the formation and function of the Pol II PIC.[5,6] Although direct physical interactions of some DNA binding transcriptional activators with selected GTFs were reported earlier,[7,8] it has remained unclear whether these interactions contribute to target gene activation.

Estrogen-related receptors (ERRα, ERRβ, and ERRγ), initially identified as factors having homology to the estrogen receptor, are physiologically important members of the NR superfamily that have been implicated in high energy-demanding biological processes as well as development and stem cell maintenance.[9–11] Unlike the case for many other NR superfamily members, the precise molecular mechanisms of transactivation by ERRs are not known. In general, direct or indirect (through NCOA/SRCs) NR interactions with p300[12,13] and direct interactions with Mediator through its MED1 subunit[14] have been identified as critical steps in ligand-dependent gene activation by the receptors. However, in the case of ERRs, which remain orphans, relevance of p300 and Mediator has not yet been studied.

Also critical for activity of many NRs, especially those involved in metabolic processes, is the cell-specific/inducible coactivator PGC-1α.[15,16] Indeed, PGC-1α-null mice show defects in various metabolic steps.[17,18] Although some NRs bind to p300 and Mediator directly, PGC-1α also binds to p300 and Mediator and synergistically enhances p300 and Mediator recruitment to DNA-bound NRs.[19,20] ERRs have been reported to display a strong dependence on PGC-1α/β for their function in cells,[9,10,18] although the underlying mechanisms are not well understood.

Here, toward understanding the precise molecular mechanisms of ERR-dependent transcription activation via PGC-1α, p300, Mediator, and potentially GTFs, we established ERR-dependent in vitro transcription assays reconstituted with DNA or chromatin templates and purified factors. We identified two pathways whereby ERRα activates transcription. In one pathway, PGC-1α mediates p300 and Mediator recruitment to promoter-bound

[1]Laboratory of Biochemistry and Molecular Biology, The Rockefeller University, New York, NY, USA. [2]Project for Cancer Epigenomics, Cancer Institute, Japanese Foundation for Cancer Research, Tokyo, Japan. [3]Department of Molecular Biology, Yokohama City University Graduate School of Medical Science, Yokohama, Japan. [4]Department of Molecular Biology and Genetics, Bilkent University, Ankara, Turkey. [5]Cancer Cell Diversity Project, NEXT-Ganken Program, Japanese Foundation for Cancer Research, Tokyo, Japan.
✉email: roeder@rockefeller.edu

Received: 7 June 2021 Accepted: 2 December 2022
Published online: 16 January 2023

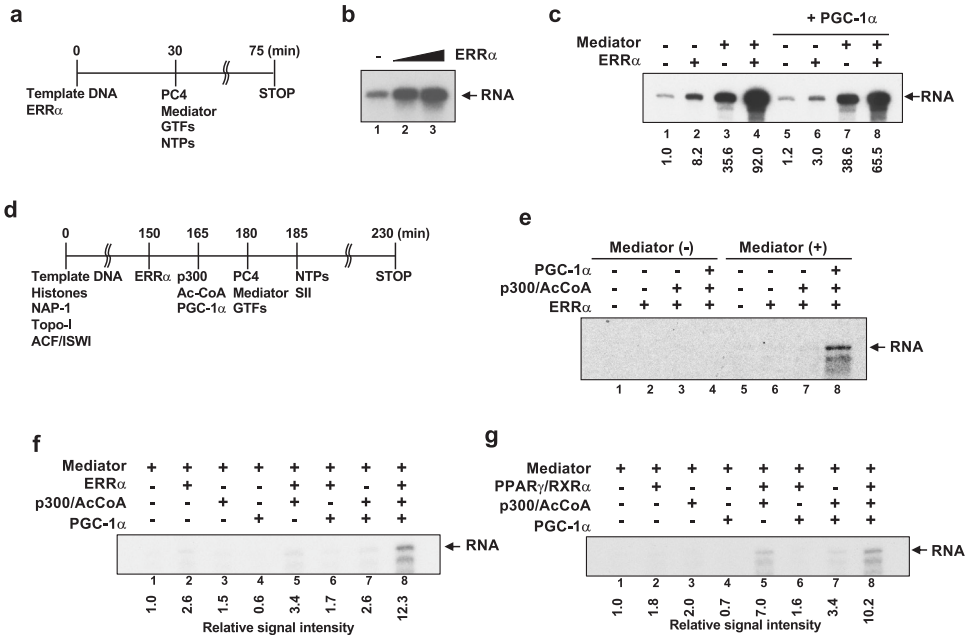

Fig. 1 ERRα-dependent in vitro transcription assays reveal cofactor-dependent and -independent activation pathways. a Schematic illustration of in vitro transcription assays with DNA templates and purified factors (shown in Supplementary information, Fig. S1). **b** ERRα-dependent transcription from a DNA template. Reactions as in **a** with 0 ng, 25 ng, and 50 ng ERRα but without Mediator. **c** ERRα-dependent, cofactor-independent transcription from a DNA template. Reactions as in **a** with components as indicated. **d** Schematic illustration of in vitro transcription assays with chromatin templates and purified components (Supplementary information, Fig. S1). **e**, **f** Mediator-, p300- and PGC-1α-dependent transcription of chromatin by ERRα. Reactions as in **d** with additions as indicated. **g** Mediator-, p300- and PGC-1α-dependent transcription of chromatin by PPARγ/RXRα. Reactions as in **d** with additions as indicated.

ERRα. The second pathway involves a direct physical interaction of GTF TFIIH, through its p52 subunit, with the DNA-binding domain (DBD) of ERRα. As validation of physiological relevance of the in vitro results, we demonstrate that ERR interactions with TFIIH and an activation function 2 (AF2)-binding cofactor (like NCOA3) are critical for expression of ERR-target genes in mouse embryonic stem cells (ESCs) and for ERRβ/γ-dependent self-renewal (maintenance) of these cells.

RESULTS

Two ERRα-dependent transcription activation mechanisms in vitro

To elucidate the molecular mechanisms of transcription activation by ERRα, we established ERRα-responsive in vitro transcription systems that were reconstituted with purified factors and DNA or chromatin templates. These systems are uniquely suited for identification of both cofactor dependencies and underlying mechanisms.[21–23] Purified human ERRα was first characterized by gel shift analysis and shown to bind to a wild-type (WT), but not a mutant, ERR recognition element (ERRE) in the human acyl-coenzyme dehydrogenase, C-4 to C-12 straight chain (*ACADM*) gene enhancer[24] (Supplementary information, Fig. S1a–c). Initial transcription assays were performed with purified ERRα, Pol II, GTFs (TFIIA, TFIIB, TFIID, TFIIE, TFIIF, TFIIH), auxiliary factor PC4, and a naked plasmid DNA template (pERRE3-HMC2AT) that contains *hACADM* ERREs (Fig. 1a; Supplementary information, Fig. S1d, e). ERRα efficiently enhanced transcription of this template (above the basal level) in a dose-dependent manner (Fig. 1b, lanes 2 and 3 vs. lane 1), but did not activate mutant templates (M1, M3) deficient in ERRα binding (Supplementary information, Fig. S1f, lanes 4 and 8). Next, we assessed the effects of (purified) presumptive ERRα coactivators PGC-1α and Mediator (Supplementary information, Fig. S1g, e), individually or in combination, in DNA-templated reactions. Surprisingly, PGC-1α did not show a stimulatory effect under these conditions but, rather, a modest inhibition of ERRα-dependent transcription (Fig. 1c, lanes 5 and 6 vs. lanes 1 and 2). Consistent with its known activities,[5,14] Mediator greatly (35.6-fold) stimulated basal (activator-independent) transcription in this system (Fig. 1c, lane 3 vs. lane 1) and amplified (11.2-fold) transcriptional activation by ERRα (Fig. 1c, lane 4 vs. lane 2) as well. The combinatorial effect of PGC-1α and Mediator on ERRα activation was also explicable, respectively, by their individual inhibitory and basal effects (Fig. 1c, lane 8 vs. lanes 2, 4 and 6).

Next, we analyzed ERRα-dependent transcription activation from a chromatinized pERRE3-HMC2AT template (Supplementary information, Fig. S1e, h). Following nucleosome assembly, templates were incubated with various combinations of ERRα and coactivators prior to transcription with purified general factors (Fig. 1d). Unlike what was seen from DNA-templated reactions, ERRα could not efficiently activate transcription in this system without any additional coactivators (Fig. 1e, lane 2 vs. lane 1). Addition of p300 (plus acetyl coenzyme) (lane 3) alone or together with PGC-1α (lane 4) did not have a marked effect on the ability of ERRα to activate the template. However, when Mediator was also included in the reactions, robust activation was observed, but only in the presence of both p300 and PGC-1α (Fig. 1e, lane 8 vs. lanes 4 and 7; see also Fig. 1f, lane 8 vs. lanes 5–7). Control experiments with purified PPARγ and RXRα (Supplementary information, Fig. S1i) showed a minimal requirement for PGC-1α (Fig. 1g, lane 8 vs. lane 5), but a strong dependence on p300 (Fig. 1g, lane 5 vs. lane 2), for activation of the cognate template. The in vitro data are thus consistent with prior reports of a strict PGC-1α requirement for ERRα-dependent, but not PPARγ/RXRα-dependent, transcription regulation in vivo.[25–28]

These results point to two ERRα-dependent transcription activation pathways. In one pathway, which was revealed through use of DNA-templated reactions, RNA polymerase II, GTFs and PC4 are sufficient. In the other pathway, which was evident with chromatin templates, coactivators PGC-1α, Mediator and p300 were essential for ERRα-dependent transcription.

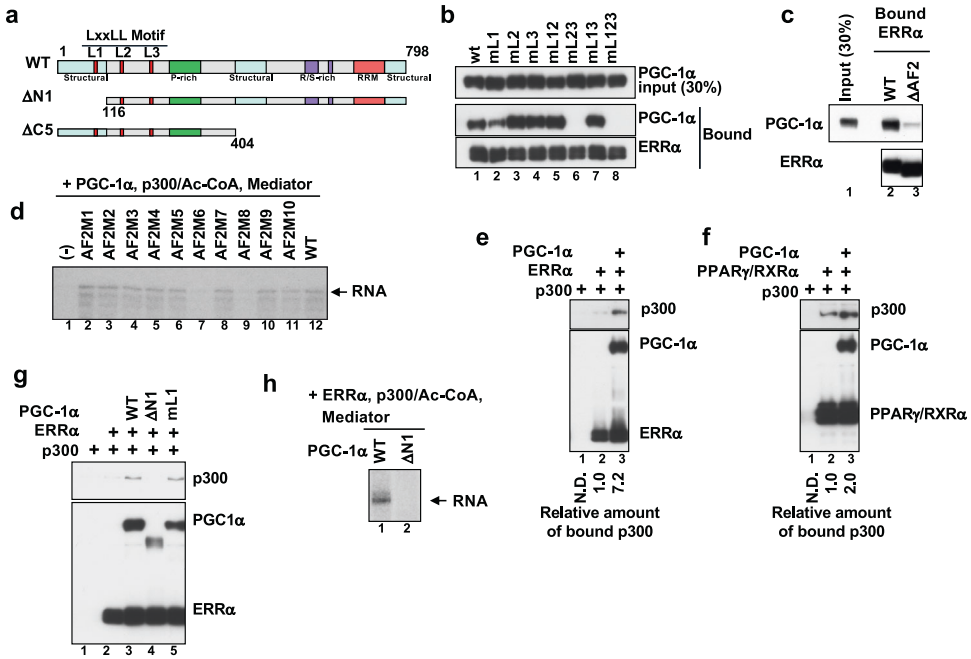

Fig. 2 p300-dependent chromatin transcription activation by ERRα is mediated by PGC-1α. a Schematic diagram of human PGC-1α and its deletion mutants ΔN1 and ΔC5. **b** PGC-1α recruitment to DNA-bound ERRα is dependent on LxxLL motifs L2 and L3. ITA with ERRE3HMC2AT DNA, ERRα, and WT or L mutant (mL) PGC-1α. Analysis by immunoblot as also in all subsequent ITAs. **c** ERRα AF2-dependent PGC-1α recruitment. ITA as in **b**, with PGC-1α and WT or ΔAF2 ERRα. **d** ERRα AF2 point mutants defective in PGC-1α-dependent chromatin transcription. Assay as in Fig. 1e with the indicated components and WT or AF2-mutated ERRα. **e** PGC-1α-dependent recruitment of p300 to DNA-bound ERRα. ITA as in **b** with the indicated components. **f** PGC-1α-independent p300 binding to DNA-bound PPARγ and RXRα. ITA with 3DR1 DNA and indicated components. **g** PGC-1α N-terminus-dependent p300 recruitment to DNA-bound ERRα. ITA with WT or ΔN1 PGC-1α as indicated. **h** PGC-1α N-terminus-dependent chromatin transcription by ERRα. Assay as in Fig. 1e with WT or ΔN1 PGC-1α.

ERRα does not bind to p300 and Mediator directly but is dependent on PGC-1α for their recruitment and transcription activation from chromatin templates

Toward understanding the strict PGC-1α requirement for activation of chromatin templates by ERRα, we used immobilized template assays (ITAs) to investigate cofactor interactions of DNA-bound ERRα. The leucine-rich motifs (LxxLL motifs) at the PGC-1α N-terminus (Fig. 2a) are known to be the major binding sites of several NRs, including ERRα.[29,30] In agreement, an ITA with WT and mutant PGC-1α showed that ERRα interacted with PGC-1α through the LxxLL motifs in PGC-1α, with apparent redundancy between LxxLL motifs 2 and 3 (Fig. 2b, lanes 6 and 8; Supplementary information, Fig. S2a). A further analysis with an ERRα deletion mutant (ERRαΔAF2) lacking AF2 domain (Supplementary information, Fig. S2b) showed a role for AF2 in interaction with PGC-1α (Fig. 2c, lane 3), consistent with earlier demonstrations of NR AF2 interactions with LxxLL motifs in various coactivators.[31,32] In an extension of earlier studies,[33] analyses of alanine-substituted ERRα point mutations in AF2 (Supplementary information, Fig. S2c, d) further established that AF2 mutations L413A/F414A (ERRα-AF2M6) and M417A/F418A (ERRα-AF2M8) eliminated PGC-1α-dependent transcription activation by ERRα (Fig. 2d, lanes 7 and 9; Supplementary information, Fig. S2e, lanes 7 and 10 vs. lane 4). A complementary ITA showed that ERRα-AF2M6 does not bind to PGC-1α (Supplementary information, Fig. S2f, lane 4). These results clearly show that physical interactions involving residues L413, F414, M417, and F418 in ERRα AF2 and residues in the second or third LxxLL motif of PGC-1α, are responsible for both the ERRα–PGC-1α interaction and the PGC-1α coactivator activity in the chromatin-templated transcription assay.

Next, the mechanism by which p300 is recruited to DNA-bound ERRα was analyzed. An ITA showed that the otherwise barely detectable interaction of p300 with DNA-bound ERRα was enhanced by 7-fold in the presence of PGC-1α (Fig. 2e, lane 2 vs lane 3). On the other hand, as reported previously,[34,35] p300 was efficiently recruited to DNA-bound PPARγ/RXRα in the absence of PGC-1α with only a modest (2-fold) enhancement by PGC-1α (Fig. 2f, lanes 2 and 3). This result is consistent with our in vitro transcription data showing only a modest effect of PGC-1α on transcription activation by PPARγ/RXRα (Fig. 1g). Consistent with a previous study,[16] a small N-terminal deletion (1–115) in PGC-1α (ΔN1; Fig. 2a; Supplementary information, Fig. S2g) resulted in loss of p300 binding in the ITA (Fig. 2g, lane 3 vs. lane 4). This was not due to the concomitant loss of the first LxxLL motif, which proved dispensable for interaction with p300 (Fig. 2g, lane 5). Consistent with its failure to interact with p300, PGC-1α-ΔN1 also did not stimulate transcription activation by ERRα in the p300-dependent chromatin-templated assay (Fig. 2h, lane 2). These results show that in contrast to the situation with PPARγ, PGC-1α is critically required for efficient p300 recruitment to DNA-bound ERRα, and thus for ERRα-dependent transcription from a chromatin template.

The ITA was also used to assess Mediator recruitment to DNA-bound ERRα. Under our assay conditions, a low level of generalized (non-specific) binding of MED1-containing Mediator to the template is sometimes observed (Fig. 3a, lane 5). This background level was not altered upon ERRα binding to the template (Fig. 3a, lane 6 vs. lane 5). However, inclusion of PGC-1α markedly increased the level of bound MED1/Mediator, reflective of authentic coactivator recruitment (Fig. 3a, lane 7 vs. lane 6). In contrast, DNA-bound PPARγ/RXRα directly and efficiently recruited Mediator without PGC-1α (Fig. 3b, lanes 7 and 9). In light of a pivotal role for MED1 in facilitating many NR–Mediator interactions, a purified Mediator preparation lacking MED1 (ΔMED1-Mediator[36]) (Fig. 3a, lane 4 vs. lane 3; Supplementary information, Fig. S2h) showed only a very weak recruitment by DNA-bound ERRα and PGC-1α in the ITA (Fig. 3a, lane 10 vs. lane 7). Consistent with this result, ΔMED1-Mediator was markedly less efficient in stimulating ERRα-dependent transcription from the chromatin template (Fig. 3c). These results

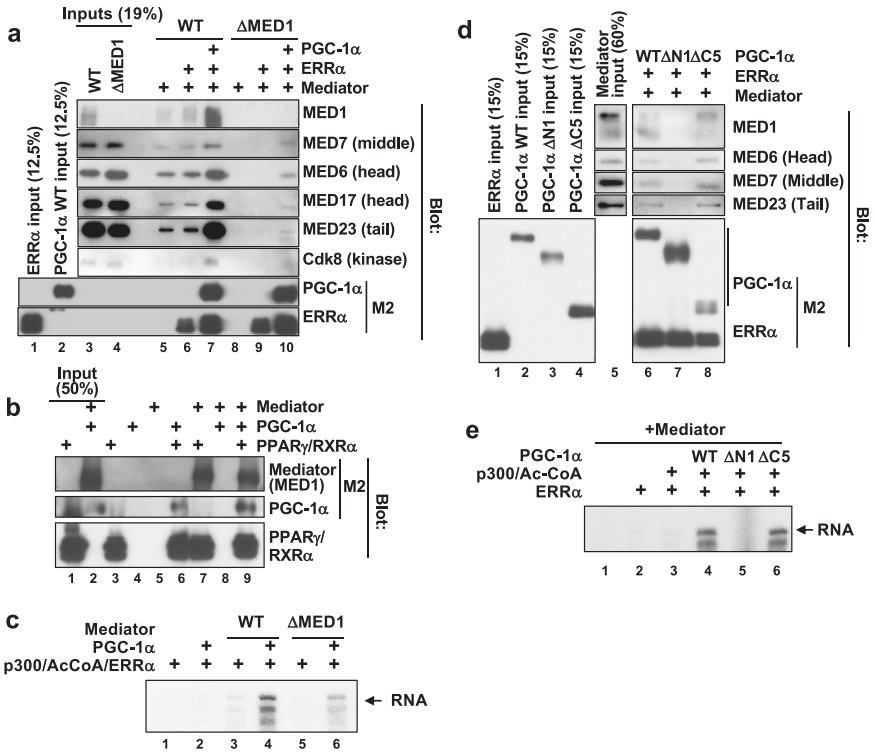

Fig. 3 Requirement of PGC-1α for ERRα-dependent Mediator recruitment via MED1 and consequent chromatin transcription activation. **a** PGC-1α-dependent Mediator recruitment, via MED1, to DNA-bound ERRα. ITA as in Fig. 2e with WT or ΔMED1 Mediator. **b** PGC-1α-independent Mediator recruitment to DNA-bound PPARγ and RXRα. ITA as in **a** with immobilized 3DR1 template. **c** MED1-dependent chromatin transcription by ERRα and PGC-1α. Assay as in Fig. 1e with WT or ΔMED1 Mediator as indicated. **d** Mediator recruitment to DNA-bound ERRα through the N-terminal half of PGC-1α. ITA as in **a** with WT and ΔC5 or ΔN1 PGC-1α deletion mutants (Fig. 2a). **e** Sufficiency of PGC-1α N-terminal half for ERRα-, p300-, and Mediator-dependent chromatin transcription. Assay as in **c** with WT and ΔC5 or ΔN1 PGC-1α deletion mutants.

show that unlike the situation for PPARγ/RXRα, PGC-1α is necessary for efficient MED1/Mediator recruitment to DNA-bound ERRα, which in turn is required for ERRα- and PGC-1α-dependent transcription activation.

We also assessed the regions of PGC-1α responsible for Mediator recruitment to DNA-bound ERRα following generation of serial deletion mutants of PGC-1α (Supplementary information, Fig. S2i). Initial GST pull-down assays showed that the N-terminal half of PGC-1α (ΔC5) is sufficient for Mediator binding (Supplementary information, Fig. S2j, lane 14 vs. lane 1) but that even a small deletion (ΔN1) of the N-terminus diminished the interaction (Supplementary information, Fig. S2j, lane 2 vs. lane 1). Although surprising in light of our demonstration[19,20] of interactions of the isolated monomeric MED1 subunit with the C-terminal half of PGC-1α, these results could reflect interactions of another Mediator subunit with the PGC-1α N-terminal domain and are also consistent with the notion of dynamic MED1–PGC-1α interactions that may be modulated by the complete Mediator complex (see Discussion).

The ERRα binding-competent PGC-1α N-terminal (ΔN1) and C-terminal (ΔC5) deletion mutants (Fig. 2a) were further tested for Mediator recruitment by ITA (see also Supplementary information, Fig. S2k for further mapping of the ERRα binding region in PGC-1α). Notably, ΔC5, but not ΔN1, clearly promoted recruitment of the Mediator complex to DNA-bound ERRα (Fig. 3d, lanes 7 and 8), consistent with the results of the direct protein–protein interaction assays (Supplementary information, Fig. S2j). Correspondingly, an in vitro chromatin transcription assay showed that ΔC5, but not ΔN1, could facilitate ERRα-dependent transcription activation (Fig. 3e, lane 6 vs. lane 5). These results establish that the N-terminal half (ΔC5) of PGC-1α is sufficient not only for ERRα binding, but also for Mediator recruitment to DNA-bound ERRα, and thus for ERRα-, PGC-1α- and Mediator-dependent transcription activation.

In conclusion, the above data suggest that unlike the situation for PPARγ/RXRα, the mechanistic basis for the strict requirement of PGC-1α for ERRα in transcriptional activation of chromatin templates in vitro lies both in ERRα's inability to directly bind critical coactivators p300 and Mediator and in PGC-1α's ability to act as an adaptor protein that facilitates these interactions.

PGC-1α- and MED1-dependent recruitment of Mediator to ERRα target genes in mouse embryo fibroblasts (MEFs)

To further verify our in vitro results, we assessed ERRα, PGC-1α, and MED1 requirements for activation of cytochrome c (*cycs*) and isocitrate dehydrogenase a (*idh3a*), which are metabolic ERRα target genes,[25,37] in MEFs, which lack detectable ERRα and PGC-1α. When ectopic ERRα and PGC-1α were jointly expressed, but not when they were expressed alone, *idh3a* and *cycs* were efficiently induced (Supplementary information, Fig. S3a). Importantly, following MED1 knockdown in these cells, the responsiveness to ERRα and PGC-1α was reduced (Supplementary information, Fig. S3a, b).

Next, recruitment of ERRα, PGC-1α and Mediator to the *cycs* and *idh3a* enhancers was monitored by chromatin immunoprecipitation (ChIP). As expected, ectopic ERRα alone was recruited to the enhancers (Fig. 4a). Ectopic PGC-1α was similarly recruited to the enhancers, but only when ERRα was co-expressed. Interestingly, whereas PGC-1α recruitment was entirely dependent on ERRα, ERRα binding to the enhancers was enhanced by PGC-1α (Fig. 4a). This PGC-1α-enhanced ERRα binding is consistent with our in vitro ITA results (Fig. 3a, lane 6 vs. lane 7 and lane 9 vs. lane 10). As also

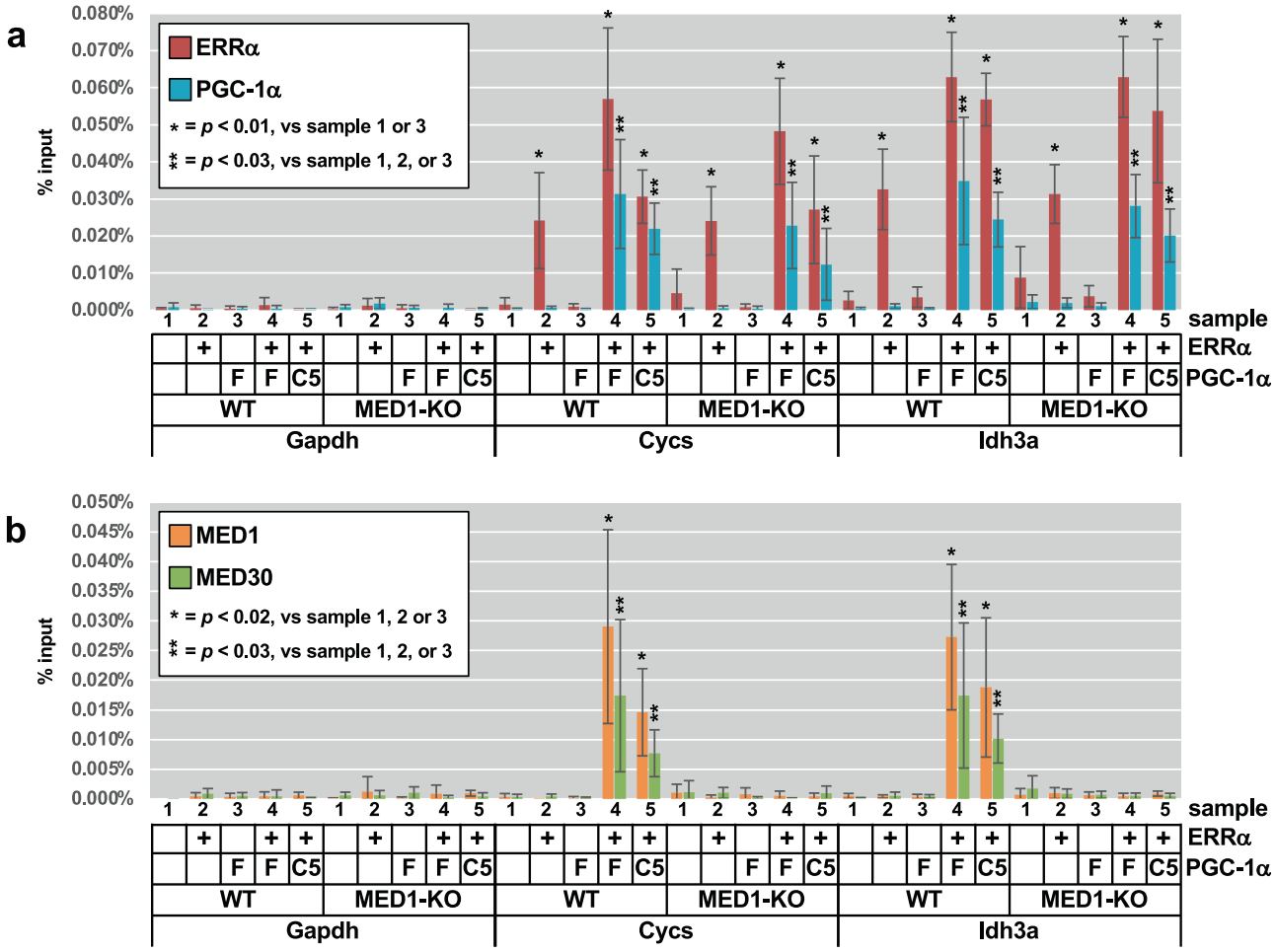

Fig. 4 Requirement of PGC-1α and MED1 for efficient Mediator recruitment and ERRα target gene expression in MEFs. a ERRα-dependent PGC-1α recruitment to ERRα target genes. ChIP assays were performed with anti-ERRα and anti-PGC-1α antibodies in MED1-KO or parental WT MEFs that overexpressed SH-hERRα and/or full-length F-PGC-1α (F) or F-PGC-1α-ΔC5 (C5) mutant as indicated. Error bars indicate standard deviations based on three independent experiments with duplicate qPCR reactions in each case. *P*-values are also shown. **b** ERRα-, PGC-1α-, and MED1-dependent Mediator recruitment to ERRα target genes. ChIP assays as in **a** with anti-MED1 and anti-MED30 antibodies.

observed in the ITA, the PGC-1α binding-deficient ERRα-AF2M6 mutant did not recruit PGC-1α in MEFs (data not shown).

As expected, binding of ERRα and PGC-1α to the enhancers was not impacted in *Med1* knockout (KO) MEFs (Fig. 4a). To assess endogenous Mediator recruitment by ChIP, we monitored both the NR-interacting, but sub-stoichiometric MED1 subunit[38] and MED30, a component of the core complex.[39] Mediator recruitment was critically dependent on both ERRα and PGC-1α (Fig. 4b). MED30/Mediator recruitment was also diminished in *Med1* KO cells, indicating that Mediator is recruited via the MED1 subunit (Fig. 4b). When WT PGC-1α and mutant PGC-1α-ΔC5, which was competent for Mediator binding and ERRα-dependent transcription in vitro, were overexpressed at comparable levels, induction levels of *cycs* and *idh3a* were essentially equivalent (Supplementary information, Fig. S3c). Similarly, the levels of ERRα-dependent recruitment of WT PGC-1α and PGC-1α-ΔC5 to the *cycs* and *idh3a* enhancers were also statistically equivalent (Fig. 4a). PGC-1α-ΔC5 also retained the ability to recruit MED1 and MED30 (and hence the Mediator) to the enhancers (Fig. 4b), consistent with the in vitro data indicating that the PGC-1α N-terminus (ΔC5) is sufficient for interaction with Mediator. These results establish that ERRα-mediated recruitment of PGC-1α (via its N-terminus) is essential for recruiting Mediator (via MED1) to ERRα-bound enhancers and consequent target gene expression. Overall, these cell-based results nicely mirror the results of the various biochemical assays above.

Taken together, the preceding results demonstrate that ERRα does not bind p300 and Mediator directly and that PGC-1α is required for efficient recruitment of p300 and Mediator to promoter-bound ERRα and ERRα-dependent transcription activation.

ERRα physically interacts with initiation factors TFIIH and TFIIB

To understand how ERRα activates transcription in the absence of coactivators, as observed in DNA-templated in vitro transcription reactions (Fig. 1), we first examined whether the ERRα AF2 was involved. Surprisingly, we found that an ERRα AF2 deletion mutant (ERRαΔAF2), which was defective in activating cognate ERRα chromatin template (Fig. 2c), activated the naked DNA-templated transcription nearly as well as the full-length protein, both in the absence (Fig. 5a, lane 3 vs. lane 2) and presence of Mediator (Fig. 5a, lane 6 vs. lane 5). The dispensability of the AF2 in this assay system further emphasizes that the observed overall stimulation of transcription by Mediator is through its direct effects on the basal machinery — potentially entailing recruitment via PIC-bound Pol II.[40] Moreover, in cell-based assays, an ERRE3 enhancer-driven reporter was also modestly induced by an ectopic ERRαΔAF2 almost as efficiently as by WT ERRα, whereas

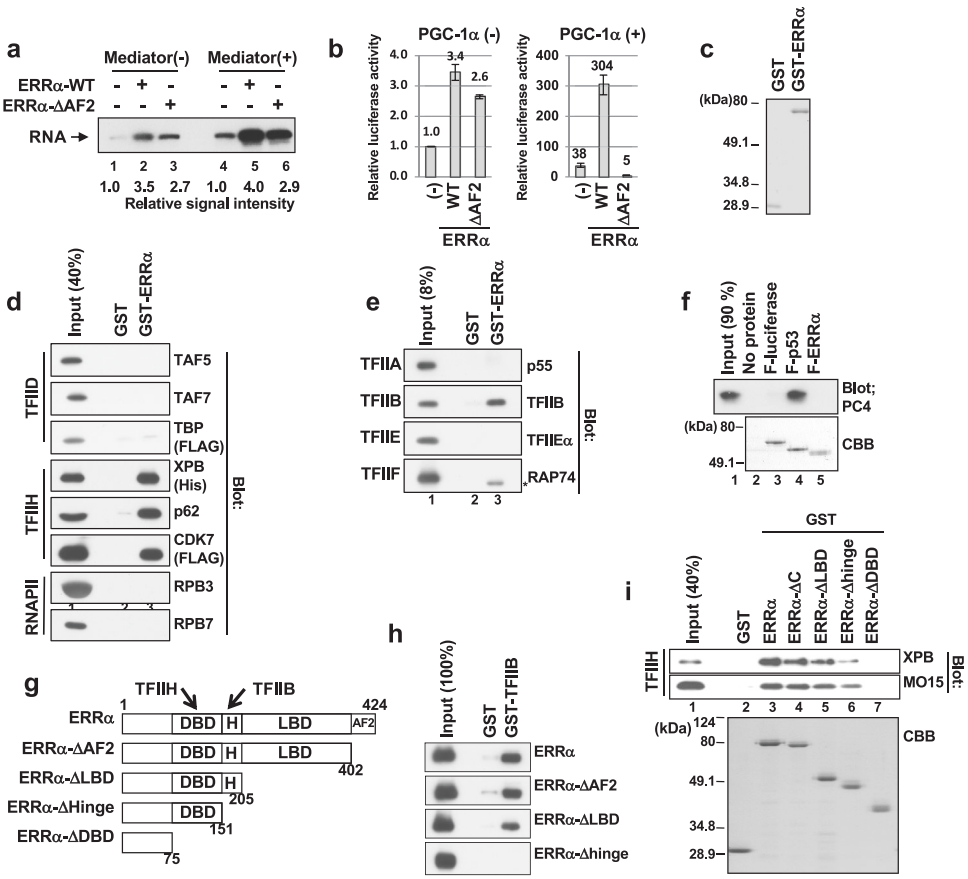

Fig. 5 Direct interactions of ERRα with TFIIB and TFIIH. a AF2-independent DNA-templated transcription by ERRα. Assays as in Fig. 1c with the indicated components. **b** Induction of an ERRα-responsive firefly luciferase reporter by ERRα-ΔAF2. 293T cells were co-transfected with the indicated expression vectors. Average activities from three independent assays are plotted as fold-increases relative to the ERRα(–)/PGC-1α(–) control. **c** SDS-PAGE analysis (Coomassie brilliant blue (CBB) staining) of recombinant GST and GST-ERRα. **d** GST pull-down assay for ERRα interactions with TFIID, TFIIH, and RNA polymerase II. Analysis by immunoblot as in all GST pull-down assays. **e** GST pull-down assay for ERRα interactions with TFIIA, TFIIB, TFIIE, or TFIIF. **f** Coimmunoprecipitation assay for ERRα interactions with PC4. Indicated proteins (top) were incubated with PC4, immunoprecipitated with M2 antibody, and monitored by immunoblotting (upper panel). SDS-PAGE with CBB staining of inputs (lower panel). **g** Schematic illustration of ERRα deletion mutants. TFIIB- and TFIIH-interacting regions of ERRα identified in **h** and **i** are highlighted. **h** GST pull-down assays for interactions of TFIIB with hERRα deletion mutants. Assay as in **e** with ERRα deletion mutants. **h** GST pull-down assays for interactions of TFIIH with ERRα deletion mutants. Assays as in **d** with hERRα deletion mutants monitored by SDS-PAGE with CBB staining. TFIIH monitored by immunoblotting of XPB and MO15 subunits.

the AF2 was nonetheless required for the more dramatic PGC-1α-dependent stimulation of reporter gene expression (Fig. 5b). These results point to a potential coactivator-independent mechanism(s) that involves a domain(s) other than the ERRα AF2 (see further below) and that might act in conjunction with the coactivator-dependent mechanism.

We next analyzed whether ERRα directly binds to the GTFs present in the DNA-templated transcription assay. Pull-down experiments utilized purified GST-ERRα (Fig. 5c) or FLAG (F)-ERRα (Supplementary information, Fig. S1b) and the individual factors (TFIIA, TFIIB, TFIID, TFIIE, TFIIF, TFIIH, RNA polymerase II, and PC4). The results (Fig. 5d–f) showed that TFIIB and TFIIH directly bound to ERRα. Pull-down assays with GST-TFIIB and serial deletion mutants of ERRα (Fig. 5g; Supplementary information, Fig. S2b) showed that TFIIB binds to ERRα-ΔLBD (lacking the ligand-binding domain) but not to ERRα-Δhinge (lacking the hinge region) (Fig. 5h). Additional pull-down assays with GST-ERRα serial deletion mutants and TFIIH showed that TFIIH bound to ERRα-Δhinge but not ERRα-ΔDBD (Fig. 5i). These results indicated that TFIIB and TFIIH bind, respectively, to the ERRα hinge (H) and DNA-binding (DBD) regions (Fig. 5g) and suggested alternative mechanisms for AF2-independent transcription activation by ERRα from DNA templates.

Interaction of ERRα with the TFIIH p52 subunit contributes to DNA-templated transcription activation in vitro by ERRα

Since TFIIB and TFIIH have general roles in PIC formation, our initial studies used DNA-templated assays (Fig. 1a) to test the functional significance of their interactions with ERRα. Assays to date have failed to show a contribution of the ERRα–TFIIB interaction to ERRα-dependent transcription (data not shown), leading us to focus on the ERRα–TFIIH interaction. Further interaction assays with purified proteins (Supplementary information, Fig. S4a) showed that the six-subunit TFIIH core complex, but not the three-subunit CDK-activating complex (CAK), bound specifically to GST-ERRα (Fig. 6a). Subsequent ITA with individually purified components of the core TFIIH complex (Supplementary information, Fig. S4b) showed selective binding of the p52 subunit (TFIIHp52) to DNA-bound ERRα, whereas TFIIHp62 binding to DNA was non-specific (Fig. 6b). As an initial indication of the significance of the ERR–p52/TFIIH interaction, the addition of monomeric p52 to the transcription assay showed only a minimal effect on basal transcription but a major (inhibitory) effect on ERR-dependent transcription, presumably due to the ability of free p52 to inhibit the ERRα–TFIIH interaction through competitive binding but not the p52 interactions within the stable TFIIH complex (Fig. 6c, lanes 4 and 6 vs. lane 2). Further studies of deletion forms

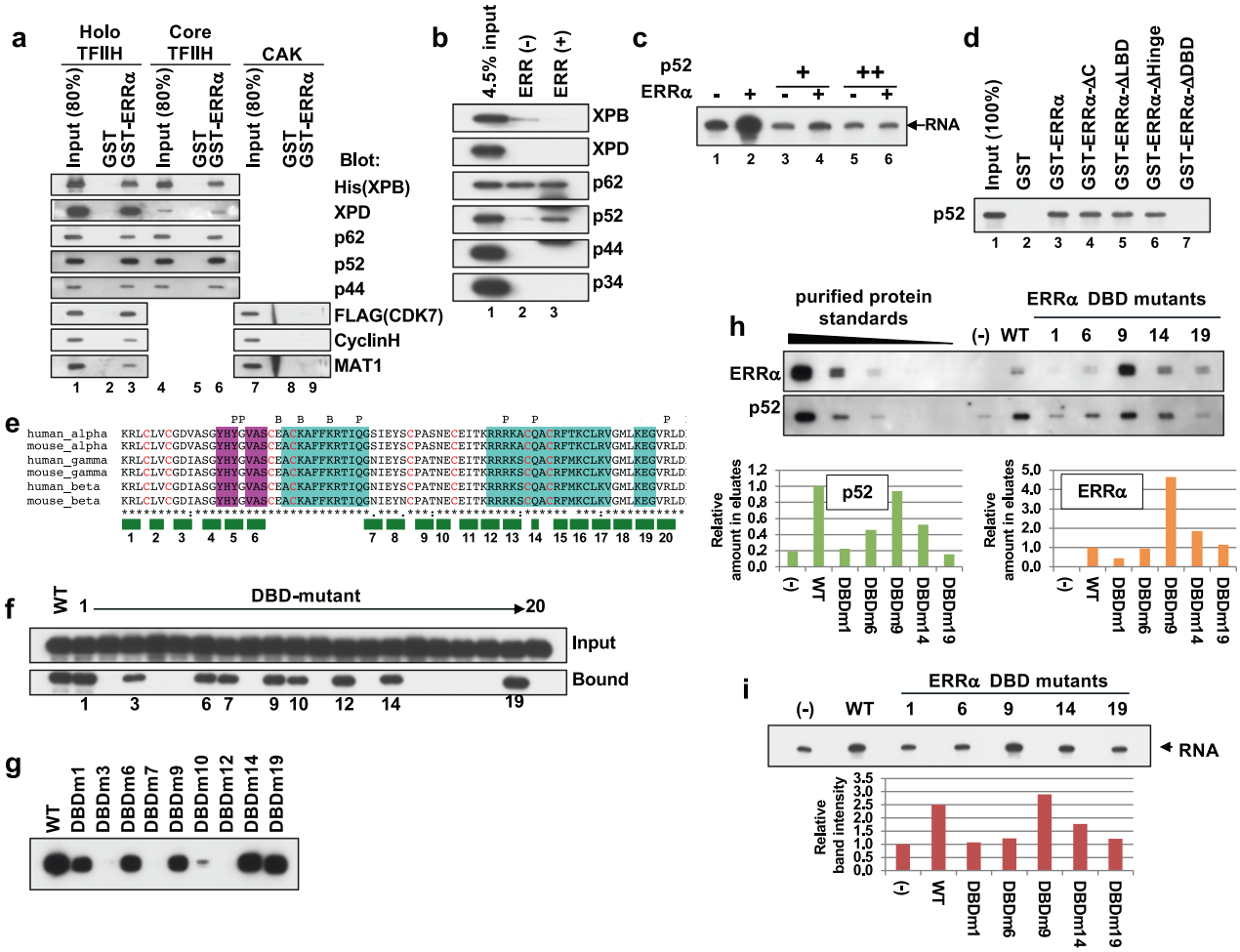

Fig. 6 Interactions with the p52 subunit of TFIIH promote DNA-templated transcription by ERRα. a Interaction of ERRα with holo TFIIH and TFIIH core. GST pull-down assays as in Fig. 5d. **b** Specific binding of TFIIHp52 to DNA-bound ERRα. ITA as in Fig. 2b using purified TFIIH subunits detected by immunoblotting with anti-FLAG M2 antibody. **c** Competitive inhibition of ERRα-dependent transcription by free TFIIHp52. DNA-templated assay as in Fig. 1b. **d** Direct interaction of the ERRα-DBD with TFIIHp52. GST pull-down assays with TFIIHp52 and hERRα serial deletion mutants as in Fig. 5i. **e** Alignment of DBDs of human and mouse ERRs. Zinc-finger cysteines are in red, and β-sheets and α-helices are in pink and blue boxes, respectively. Residues in direct contact with a base (B) or the phosphate backbone of DNA (P)[41] are indicated. Residues mutated to alanine in the DBD region (ERRα-DBDm) are numbered and identified by a green bar underneath. **f** Screening for DNA binding-competent ERRα-DBD mutants. ITA as in Fig. 2b, with lysates containing bacterially expressed F-hERRα-DBD mutants, under less stringent conditions (no carrier DNA, see Materials and Methods). **g** Analysis of DNA-binding abilities of purified hERRα-DBD mutants (ERRα-DBDm). ITA as in **f**. **h** Identification of ERRα-DBD mutants deficient in TFIIHp52 binding. ITA as in **b** under more stringent conditions (see Materials and Methods). Bound proteins were detected by immunoblot and relative amounts (lower two panels) were estimated from standard curves (left 5 lanes in each panel). **i** Elimination of ERRα-dependent transcription from DNA templates by DBDm6/19 mutations. Assays as in **c**, with the indicated mutants.

of TFIIHp52, analyzed in the context of reconstituted TFIIH, failed to identify mutations that selectively inhibit ERR-dependent transcription relative to basal transcription (data not shown), leading us to focus on an ERR mutagenesis approach to establish the functional significance of the ERRα–TFIIH interaction.

As observed with the holo-TFIIH complex, GST pull-down assays with GST-ERRα serial deletion mutants (Fig. 5i) showed that TFIIHp52 bound to the DBD of ERRα (Fig. 6d). We therefore sought to identify ERRα DBD mutants that were selectively deficient in binding to TFIIHp52 and suitable for assessing the requirement of the TFIIHp52–ERRα interaction for DNA-templated transcription activation. Because it was expected that mutations within the DBD might affect the DNA-binding ability of ERRα, serial point mutations were carefully introduced into the DBD (ERRα-DBDm, Fig. 6e) but avoiding cysteine residues that are part of zinc-finger motifs and amino acids that make direct contacts with DNA.[41] ITAs showed that several mutants (DBDm1, 6, 9, 14, and 19), when purified, retained DNA-binding abilities at levels comparable to that of WT ERRα (Fig. 6f, g; Supplementary information, Fig. S4c). Further ITAs under very stringent conditions (high detergent concentrations) to more clearly reveal mutant TFIIHp52 binding deficiencies indeed showed variable binding efficiencies, with ERRα-DBDm6 and ERRα-DBDm19 binding comparably, ERRα-DBDm9 and ERRα-DBDm14 binding more strongly, and ERRα-DBDm1 binding more weakly relative to WT ERRα (Fig. 6h, top panel). A parallel analysis of TFIIHp52 recruitment showed significant decreases (relative to WT ERRα) with ERRα-DBDm6 and ERRα-DBDm14 and almost complete loss (near background levels) with ERRα-DBDm1 and ERRα-DBDm19 (Fig. 6h, bottom panel). These results identify ERRα-DBDm6 and ERRα-DBDm19 as TFIIHp52 binding-deficient mutants that retain normal (WT) DNA-binding ability. Notably, the residues mutated in ERRα-DBDm6 and ERRα-DBDm19 are evolutionarily conserved (Supplementary information, Fig. S4d) and closely positioned along the outer

surface of the DBD.[41] Finally, DNA-templated transcription assays with these mutants showed that ERRα-DBDm1, ERRα-DBDm6, ERRα-DBDm14, and ERRα-DBDm19 did not activate transcription with the GTFs while ERRα-DBDm9 activated as well as WT ERRα (Fig. 6i). Importantly, the transcription activation potential of each mutant corresponded well with the amounts of TFIIHp52 recruited to DNA-bound ERRα in ITA. Additional analyses of ERRα-DBDm6 and ERRα-DBDm19 failed to reveal any effects of the mutations on various ERRα parameters, including dimerization,[42] PGC-1α binding, and selected post-translational modifications[9] (Supplementary information, Figs. S2f and S4e–h). In conclusion, the data demonstrate that direct physical interactions between TFIIHp52 and distinct residues in the ERRα DBD underlie activation of DNA-templated transcription.

ERRβ and ERRγ have similar TFIIHp52/coactivator dependencies as ERRα

The preceding analyses clearly showed that ERRα activates transcription in vitro through both PGC-1α and TFIIHp52 interactions. Toward elucidating the biological significance of these mechanisms, and given the high homology between ERR family members, whose roles in cells may be either redundant or mutually exclusive with that of ERRα,[43] we compared ERRβ and ERRγ to ERRα in our assays. Like ERRα, both short (S) and long (L) forms of ERRβ and ERRγ efficiently activated transcription in chromatin-based assays in a PGC-1α- and p300-dependent manner (Supplementary information, Fig. S5a–c). Amino acids corresponding to those mutated in ERRα-AF2M6 are conserved between all human and mouse ERRs (Supplementary information, Fig. S5d). We found that mutation of these residues also disrupted interactions of ERRβ and ERRγ with PGC-1α (Supplementary information, Fig. S5e, f). GST pull-down assays showed that ERRβ and ERRγ bound to TFIIH and TFIIB as efficiently as ERRα (Supplementary information, Fig. S5g–i). Amino acids corresponding to those mutated in ERRα-DBDm6 and ERRα-DBDm19 were also conserved among human and mouse family members (Fig. 6e). As observed above for human ERRα, an ITA showed that human and mouse ERRα, ERRβ and ERRγ, as well as corresponding hERRα-DBDm6- and hERRα-DBDm19-related derivatives, bound to the ERRE, whereas ERRα-DBDm3-related derivatives did not (Supplementary information, Fig. S5a, j). Moreover, DBDm3, DBDm6, and DBDm19 mutants of human ERRβ and ERRγ, as well as of mouse ERRα, ERRβ, and ERRγ, displayed variable diminished abilities to activate DNA-templated transcription in vitro (Supplementary information, Fig. S5k). Finally, as for ERRα (Fig. 6c), the purified TFIIHp52 competitively inhibited transcriptional activation by hERRβ, hERRγ, mERRα, mERRβ, and mERRγ in DNA-templated reactions (Supplementary information, Fig. S5l, m). We therefore conclude that ERRβ/γ utilize PGC-1α- and TFIIHp52-dependent activation pathways through interactions entailing conserved amino acid residues. We also note a recent report[44] of an ERRβ–Mediator interaction, which indicates a potentially modified mechanism for Mediator recruitment by ERRβ but, at the same time, does not rule out roles for PGC-1α in facilitating Mediator (and p300) recruitment to ERRβ target genes.

ERRβ/γ binding to ERREs, TFIIHp52 and AF2-binding coactivators is required for efficient ESC self-renewal maintenance

ERRβ is critical for maintenance of mouse ESC self-renewal under 2-inhibitor ("2i") conditions, but dispensable in the presence of leukemia inhibitory factor (LIF; "2iL").[10] ESCs thus provided a convenient biological system to evaluate the significance of our findings of physical and functional interactions of ERRs with TFIIHp52 and with AF2-binding cofactors that include NCOA3, which is an essential cofactor for ERRβ.[45] ITA showed that NCOA3 bound selectively to ERRβ and ERRγ (but not to ERRα), while NCOA1/2 bound all isoforms of ERRs, and that AF2M6 mutants of all isoforms lost NCOA1/2/3-binding ability (Supplementary information, Fig. S6g, h). Moreover, as with ERRα and PGC-1α (Fig. 3), NCOA3 directly bound to Mediator and facilitated Mediator recruitment to DNA-bound ERRβ and ERRγS (Supplementary information, Fig S6i, j). These results indicate that NCOA3 can function similarly to PGC-1α in Mediator recruitment.

Using CRISPR/Cas9 approaches, we established ERRβ-KO ESCs (Supplementary information, Fig. S6a, b). KO cells were further engineered to inducibly express ectopic ERRβ (KO/ERRβ-wt clones) at levels comparable to endogenous ERRβ in parental ESCs (WT cells, Supplementary information, Fig. S6f). As previously reported,[10] colony formation assay (CFA) of WT/mock and KO/mock cells (mock refers to treatment with control lentivirus) showed that the colony formation ability of ERRβ-KO cells, and hence their ability to self-renew, was severely diminished under 2i conditions but minimally impacted under 2iL conditions (Fig. 7a; Supplementary information, Fig. S6d). Importantly, when ectopic ERRβ expression was induced in KO/ERRβ-wt clones by doxycycline (Dox) (2i/Dox(+)), the colony formation ability was restored to the level seen under 2iL/Dox(–) conditions. The colony formation ability of uninduced KO/ERRβ-wt cells in 2i medium (2i/Dox(–)) remained similar to that of KO/mock cells grown under 2i conditions (Fig. 7a; Supplementary information, Fig. S6d). These results confirmed the suitability of this ERRβ knockout and rescue system for evaluating the function of ERRβ interactions in ESCs.

We also generated KO cells that inducibly express ERRβ mutants deficient in binding to ERRE (KO/ERRβ-DBDm3 clones), TFIIH (KO/ERRβ-DBDm6 and KO/ERRβ-DBDm19 clones), or AF2-binding cofactors (i.e., PGC-1α and NCOA3) (KO/ERRβ-AF2M6 clones). CFA results showed that relative to their growth in 2iL/Dox(+) conditions, KO/ERRβ-DBDm3 and KO/ERRβ-AF2M6 clones were severely (~10% and ~30%, respectively) compromised in their ability to form colonies under 2i/Dox(+) conditions (Fig. 7b). Moreover, the colony formation abilities of KO/ERRβ-DBDm6 and KO/ERRβ-DBDm19 clones in 2i/Dox(+) were also decreased to ~50% and ~75%, respectively, relative to the 2iL/Dox(+) condition (Fig. 7b). Concomitantly, under 2i/Dox(+) conditions, expression levels of pluripotency marker genes *Nanog*, *Rex1*, *Klf4*, and *Tbx3*, but not *Sox2, Nr5a2* and *Oct3/4*, were markedly decreased in KO/ERRβ-mutant clones just as in the KO/mock clones. By contrast, in KO/ERRβ-wt clones the expression levels of these genes were nearly completely restored (Fig. 7c). Overall, these results indicate that ERRβ interactions with ERREs, TFIIHp52 and AF2-binding cofactors (i.e., PGC-1α and NCOA3) play significant physiological roles in expression of genes important for self-renewal maintenance of ESCs.

Quantitative PCR (qPCR) analysis showed that in ESCs only ERRβ was highly expressed, with ERRα being weakly expressed (< 20% of ERRβ expression) and ERRγ being barely detectable (Supplementary information, Fig. S6e). Interestingly, CFAs of KO cells expressing either ERRα or ERRγ (KO/ERRα-wt or KO/ERRγ-wt clones) showed that ERRγ-wt, but not ERRα-wt, significantly compensated for ERRβ loss under 2i/Dox(+) conditions (Fig. 7d), indicating that ERRγ is functionally redundant with ERRβ in ESCs. CFAs with KO cells expressing mutant forms of ERRγ (KO/ERRγ-DBDm3, KO/ERRγ-DBDm6, KO/ERRγ-DBDm19, and KO/ERRγ-AF2M6 clones) showed that, like their ERRβ counterparts, these mutant KO/ERRγ clones also had compromised colony formation abilities under 2i/Dox(+) conditions, indicating that ERRγ interactions with ERREs, TFIIH, and AF2-binding cofactors (PGC-1α and NCOA3) are critical for ERRγ function and facilitate its rescue of ERRβ loss in ESCs (Fig. 7e). Notably, the result that ERRβ/γ, but not ERRα, interacts with NCOA3 (Supplementary information, Fig. S6h) provides an explanation for the inability of ERRα to substitute for ERRβ (and ERRγ) under 2i/Dox(+).

The above results suggested the feasibility of confirming the functional significance of the ERRβ interactions with ERREs, TFIIHp52 and AF2-binding cofactors (PGC-1α and NCOA3) in ESCs by assessing the abilities of WT and mutant forms of ERRβ (or

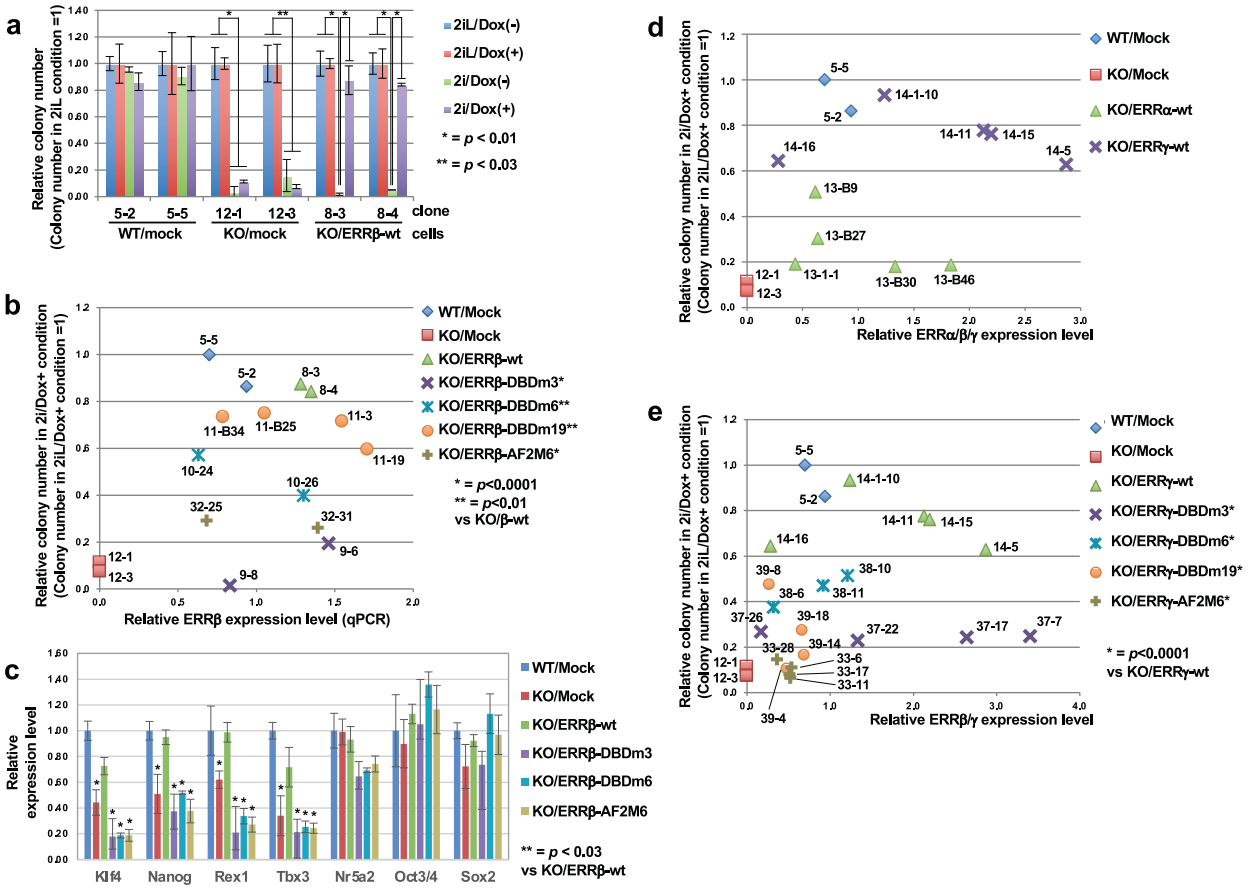

Fig. 7 Requirement of ERR–TFIIHp52 interactions for efficient ERRβ/γ-dependent maintenance of ESC self-renewal. a Diminished colony formation ability of ERRβ-KO ESCs and rescue by ectopic (dox-induced) ERRβ expression. CFA was performed twice for each clone under the indicated conditions (see also Supplementary information, Fig. S6d). *P*-values are also shown. **b** Incomplete rescue of colony formation defect of ERRβ-KO cells by TFIIH binding-deficient ERRβ mutants. Indicated clones (key on right side) were subjected to CFA as in **a**. Data for the mutant clones are plotted together with data from **a**. Relative expression levels of ERRs were determined by RT-qPCR. **c** Effects of ERRβ WT and DBD mutants on rescue of pluripotency gene expression in ERRβ-KO ESCs. WT, KO and KO cells ectopically expressing ERRβ WT or ERRβ mutants (indicated on the right) were cultured under 2i/Dox(+) conditions for 3 days. Mean relative expression levels of the indicated genes from duplicated RT-qPCR analyses for two independent experiments, each with two clones (see **b**) are shown; the standard deviations with error bars and *P*-values are shown. **d** ERRγ, but not ERRα, rescues the colony formation deficiency of ERRβ-KO cells. WT, KO and KO clones expressing ERRα or ERRγ were subjected to CFA as in **c**. Panel **c** data for WT/mock and KO/mock clones are included for reference. **e** Attenuated rescue of colony formation deficiency of ERRβ-KO cells by TFIIH binding-deficient ERRγ-DBDm6 and -DBDm19. WT, KO and KO cell clones expressing the indicated ERRγ mutants were subjected to CFA and analyzed as in **d**.

ERRγ) to rescue the colony formation activity of ERRβ-KO cells. Toward this objective, we next determined the gene expression profiles of WT/mock, KO/mock, KO/ERRβ-wt, KO/ERRβ-mutant, and KO/ERRγ-wt clones grown under 2i/Dox(+) conditions by RNA-seq analyses (Fig. 8a). By filtering genes whose differential expression levels (WT/mock vs. KO/mock) were restored upon ectopic expression of ERRβ-wt in KO/ERRβ-wt, a total of 3634 up-regulated and 3325 down-regulated ERRβ target genes were identified (Fig. 8a; Supplementary information, Table S1). Gene ontology (GO) enrichment analysis of each gene set showed that ERRβ predominantly up-regulated various metabolic/catabolic genes, including fat/lipid metabolism genes, as reported for all ERR family members (Fig. 8b).[10] Not reported previously is the finding that ERRβ also predominantly up-regulated various genes associated with microtubule/cilia-related cellular functions and down-regulated genes associated with RNA metabolism (Fig. 8b, c). Towards gauging the extent of dependency of individual genes on one or more of the mechanisms described herein, the identified up-regulated genes were classified based on their expression levels in individual clones that expressed ERRβ mutants ERRβ-DBDm3, ERRβ-DBDm6, and KO/ERRβ-AF2M6, which, respectively, eliminate interactions with the ERRE, TFIIH, and PGC-1α and NCOA3 cofactors (Fig. 8d; Supplementary information, Table S1). Consistent with the general model proposed based on our in vitro assays, most ERRβ target genes fell into a group that could not be rescued by all three mutants (class 1, 61.4%), indicating joint dependency on ERRβ interactions with ERRE, TFIIH, and AF2-binding cofactors. The second largest group, although much less extensive than class 1 (class 8, 21.9%), contained genes that were rescued by all three mutants, indicating, surprisingly, that none of the above mechanisms was necessary for their expression (but see Discussion). The groups not rescued by the ERRE-binding mutant (classes 3 and 4) were smaller but had significant numbers of target genes, in line with the more basic requirement of interactions with the ERRE relative to the other two interactions. Importantly, the percentage of target genes dependent on each mechanism (Fig. 8e) was negatively correlated with the colony formation ability of clones expressing corresponding mutants (Fig. 7b). Interestingly, each of the classes, which are individually representative of the different mechanisms, included gene sets with significantly different biological functions (Supplementary information, Fig. S6k). For example, class 1 (ERRE/TFIIH/cofactor-binding dependent) was relatively enriched with metabolism- and migration-related genes, while class 8 (ERRE/TFIIH/cofactor-

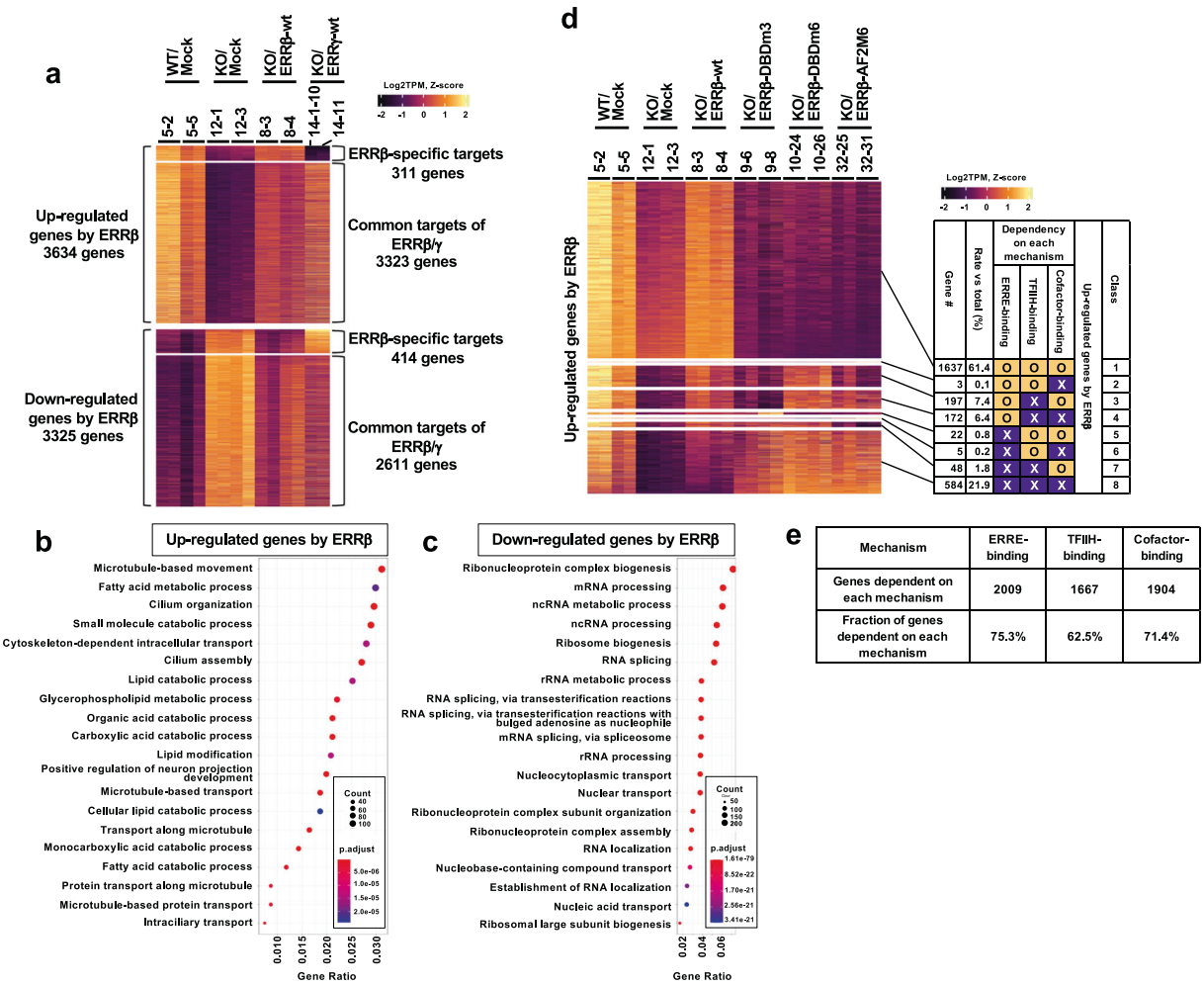

Fig. 8 Identification of ERRβ/γ target genes in ESCs and their dependency on interactions with ERRE, TFIIHp52, and AF2-binding cofactors. a Identification of ERRβ and ERRβ/γ target genes. WT, KO, and KO cell clones expressing ERRβ-wt or ERRγ-wt were analyzed by RNA-seq, and the expression levels of identified target genes were represented with a heatmap. **b** GO enrichment analysis of up-regulated ERRβ target genes. Enriched GOs with top 20 ratios are shown with gene counts and adjusted *P*-values as indicated. **c** GO enrichment analysis of down-regulated ERRβ target genes as in **b**. **d** Classification of up-regulated ERRβ target genes. ERRβ up-regulated target genes were classified according to the recovery of gene expression by each mutant. Number and percentages of genes in each class are also represented. **e** Percentages of ERRβ target genes dependent on each mechanism.

binding independent) included cytoskeleton-related genes. These results indicate that the gene activation pathways of ERR (ERRE/TFIIH/cofactor-binding) are selectively utilized for specific gene sets. Only a small fraction of ERRβ target genes were not rescued by ERRγ (8.6% and 12.5% genes among the up-regulated and down-regulated genes, respectively) (Fig. 8a; Supplementary information, Table S1). GO enrichment analysis further showed enrichment of metabolism-related genes among the genes commonly up-regulated by ERRβ/γ. However, gene sets regulated exclusively by ERRβ were enriched for genes controlling DNA checkpoint, cell junction, and protein localization (Supplementary information, Fig. S6l); these genes were not picked up when GO analysis of the entire ERRβ target gene set was done (Fig. 8b). On the other hand, gene sets that were down-regulated either commonly by ERRβ and ERRγ or specifically by ERRβ showed enrichment of similar RNA function-related genes (Supplementary information, Fig. S6m).

To explore the mechanisms whereby genes might be differentially regulated by individual ERRβ interactions (ERRE, TFIIH, cofactors PGC-1α/NCOA3), we analyzed publicly available data sets for enrichment of motifs around ERRβ-binding sites in ESCs. We focused on motifs that would be enriched at regions known to bind "WT" ERRβ within ±50 kb from the transcription start site (TSS) of genes of each class (see Materials and methods; Supplementary information, Fig. S6n and Table S2). As expected, motifs similar to the canonical ERRE were top ranked in all classes because they are identified as ERRβ-binding regions. Nonetheless, the analysis provided several interesting insights. First, although the core sequence (AAGGTCA) of the ERREs was nearly identical in all classes, adjoining 1–3 bp sequences varied significantly. Second, motifs for Klf family members, which were reported as the pivotal activators for naïve pluripotency of ESCs, were secondarily enriched in all groups, while motifs for other pluripotency-related activators, i.e., Oct and Sox, were differentially detected among the classes.[46] Various other transcription factor-binding motifs were also differentially enriched among the classes; e.g., TEAD4 and BBX were specifically enriched in classes 1 and 8. Thus, although ChIP-seq analyses with individual mutants remain to be performed to dissect the precise mechanism of DNA/TFIIH/AF2-independent ERRβ target gene regulation, various extended ERREs and binding sites for pluripotency-related, as well as other, activators might account for differential functional dependency of ERR-dependent genes on the various pathways in ESCs (see Discussion).

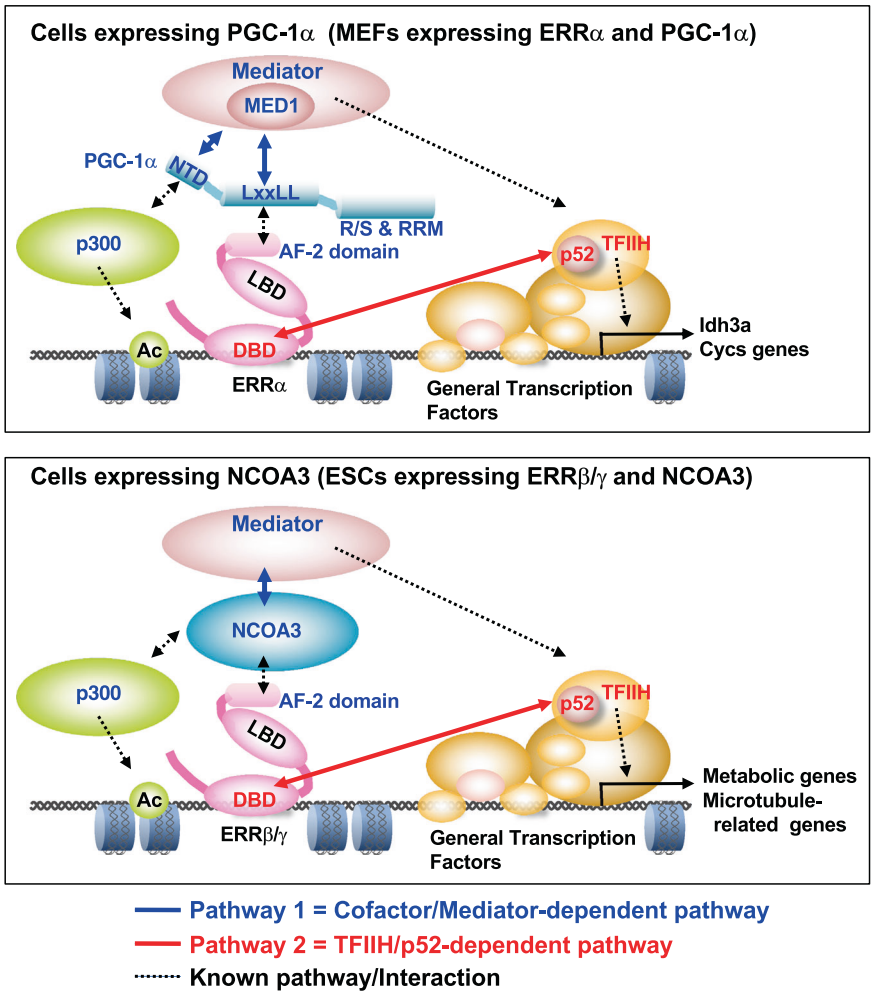

Fig. 9 ERR activates transcription through two different pathways. Pathway 1 (blue arrow): in the case of cells expressing PGC-1α (e.g., MEFs, upper panel), the AF2 region of a DNA-bound ERR binds to LxxLL motifs 2 and 3 of PGC-1α, whose N-terminal half in turn facilitates the recruitment of p300 and MED1-containing Mediator. Alternatively, in the case of cells lacking PGC-1α (e.g., ESCs, lower panel), the AF2 region of a DNA-bound ERR binds to NCOA3, which facilitates the recruitment of Mediator and likely p300 as well.[13] Histone acetylase p300 facilitates chromatin remodeling and Mediator directly promotes PIC formation (blue dashed line). Pathway 2 (red arrow): the DBD of DNA-bound ERR interacts with the p52 subunit of GTF TFIIH, thereby impacting its transcription initiation functions (red dashed arrow). Both pathways can operate simultaneously to activate transcription on individual target genes.

In summary, the diverse interactions of ERRβ with ERREs, TFIIH, and AF2-binding cofactors (PGC-1α and NCOA3) represent physiologically important mechanisms that are critical for ERR functions in maintaining the self-renewal ability of ESCs but are variably required for different target genes.

DISCUSSION

Although the study of transcription activation mechanisms historically began with identification of GTF targets of selected activators, the predominant roles of coactivators was soon realized and emphasis shifted to an understanding of their mechanisms. In this study we used both reconstituted in vitro transcription and cellular and ESC genetic analyses to reveal molecular mechanisms (beyond DNA binding) whereby ERR family members regulate target gene expression. Our data point to two mechanistic pathways for DNA-bound ERRs, one via interaction with GTF TFIIH and the other via interaction with the AF2-binding cofactors PGC-1α and NCOA3, which in turn interact with and facilitate functions of general coactivators (Mediator, p300; Fig. 9). Thus, at least for a subset of transcriptional activators, both GTFs and coactivators are critical mechanistic targets.

ERR- and PGC-1α-dependent transcription activation

Consistent with results of cell-based studies,[25–28] our in vitro chromatin transcription assays showed that activation by ERRα is strongly dependent on PGC-1α. Whereas we found no direct physical interactions between ERRα and the coactivators p300 and Mediator, unlike the case for many other NRs, biochemical analyses showed that the PGC-1α dependency results from its ability to directly facilitate recruitment of Mediator and p300 to template-bound ERRα. PGC-1α has been suggested to act like a "protein ligand" for orphan ERRs because of specific binding between ERR AF2 and the PGC-1α LxxLL motif and a corresponding strong requirement for ERR target gene activation.[47,48] We here provide further evidence, as well as a potential mechanism, to support the notion of PGC-1α as a protein ligand. Thus, analogous to what ensues upon binding of small-molecule ligands to cognate NRs, p300 and Mediator sequentially interact with ERRs only after PGC-1α binds to ERRs. Whether PGC-1α fulfills this role by inducing ERR conformational changes, similar to authentic ligands, or by serving as a scaffold for the recruitment of the cofactors (as seems likely from the observed interactions) remains to be investigated.

Overall, we envision a general multi-step pathway for ERR target gene activation involving (i) ERR binding to ERREs, (ii) ERR

recruitment of PGC-1α, (iii) PGC-1α-mediated recruitment of p300 to effect chromatin opening, likely in conjunction with other chromatin cofactors, and (iv) PGC-1α-mediated recruitment of Mediator to facilitate PIC formation and function. In this regard, our finding that Mediator recruited to ERR target genes contains (and requires) the MED1 subunit, which anchors many other direct NR–Mediator interactions, has interesting mechanistic implications. With a wide range of newly described effector functions, Mediator's role is not simply to facilitate formation of the PIC but also to fine-tune its function at post-recruitment stages.[5,6] Although our data do not allow us to conclude whether any direct contacts between ERRs and MED1 are ultimately established, the selection of otherwise sub-stoichiometric MED1-containing Mediator complexes[38] implies that Mediator effector functions that might preferentially be induced via this subunit are relevant for ERR activity.

We previously suggested that, through dynamic interactions between the C-terminal RNA-binding and RS domains of PGC-1α and its MED1 subunit, Mediator might coordinate the chromatin remodeling and PIC formation steps.[19,20] The C-terminal region of PGC-1α has also been reported to regulate RNA processing,[49] as well as to modulate PGC-1α coactivator activity through post-translational modifications.[50,51] In the present study, focusing on interactions of template-bound ERR, we identified additional critical roles for the N-terminal region of PGC-1α in Mediator-dependent gene activation by ERR. Indeed, a PGC-1α deletion mutant (ΔC5) that lacks the RNA-binding region and the RS domain, retained full capability of binding to ERRα and Mediator and activating genes. Although these results might be a reflection of the dynamic nature of PGC-1α interactions, or of additional PGC-1α interactions with other Mediator subunits, they also highlight a potential dispensability of the C-terminal half of PGC-1 in certain scenarios, as also suggested by the existence of functional isoforms lacking these domains.[52]

TFIIH as an ERR activation target

Our study also revealed direct physical interactions between ERRs and TFIIH that were functionally critical both in vitro and in ESCs. Although several transcription factor–TFIIH interactions have been reported (Supplementary information, Table S3), possible functional effects, including transcription factor phosphorylation by TFIIH (see below), are largely unexplored. Even in the exceptional cases of xeroderma pigmentosum and trichothiodystrophy,[53–56] where TFIIH subunits (XPB, XPD, p62, CAK) have been implicated in these pathologies (Supplementary information, Table S3), there has been no clear-cut identification of specific transcription factor-interacting TFIIH subunits. This likely reflects the inherent difficulty in maintaining the essential function of a GTF such as TFIIH in global transcription while assessing (by mutation) its gene-specific functions through interactions with distinct activators. Here, by uniquely combining biochemical and genetic analyses and taking advantage of identified ERR DBD mutants that are selectively defective in GTF (TFIIH) interactions relative to other activator functions, we have clearly established: (i) direct binding of ERRs to TFIIHp52; (ii) ERR domains and residues selectively required for TFIIHp52 binding; (iii) the importance of the TFIIH–ERRβ interaction for activation of select ERRβ target genes in ESCs; and (iv) a corresponding requirement of the TFIIH–ERRβ/γ interaction for ESC self-renewal. We also report, for the first time, that by targeting a general initiation factor, an NR DBD can execute an activating function. Notably, our approach of identifying interactions of immobilized DNA-bound ERR that may have undergone significant conformational changes,[41,57,58] and eliminates non-specific cofactor interactions through the DNA-binding surface of the DBD, was instrumental in revealing this unusual interaction.

How TFIIH binding results in activation of ERR-dependent genes remains unclear. Reports that various activators, including NRs, are phosphorylated by TFIIH CAK[56,59,60] suggested that CAK-dependent phosphorylation of ERR might modulate its activity. However, we found that ERRα phosphorylation efficiency (by TFIIH) was very low (< 1%) and did not affect ERRα-dependent transcription in vitro (Supplementary information, Fig. S4i–m). Because p52 modulates TFIIH/XPB ATPase activity required for promoter opening and promoter escape,[61–63] the ERRα–TFIIH interaction might yet regulate these TFIIH activities, potentially in concert with the Mediator.[64]

Variable requirements for the functions of ERRβ interactions with ERREs, TFIIH and AF2-binding factors in ESCs

It has been reported that ESCs are deficient in PGC-1α and PGC-1β (although they do contain the family member PRC) and are dependent on another cofactor (NCOA3/SRC3) that also interacts with the ERRβ AF2 in ESCs.[45] We now show that NCOA3, like PGC-1α, can facilitate Mediator recruitment to DNA-bound ERRβ/γS through a direct interaction with Mediator (Supplementary information, Fig. S6i, j). Moreover, the ERRβ/γS AF2M6 mutant that is defective in binding PGC-1α is also defective in binding NCOA3 (Supplementary information, Fig. S6h). Thus, NCOA3 is a functional analog of PGC-1α (see above) and, given further its predominance in ESCs, the ERRβ/γS AF2M6 mutant thus served as a good proxy for assessing the roles of ERR–NCOA3 interactions in our genomic analyses of ERR-dependent gene regulation in ESCs.

In particular, our detailed analyses of ERRβ function in ESCs helped determine whether the activation pathways dependent, respectively, on interactions with TFIIH and the AF2-binding cofactor (probably NCOA3) operate independently or cooperatively. A large number of ERRβ target genes were identified by RNA-seq analysis and, based on complementation experiments, were grouped into 8 classes based on dependency on a given interaction (ERRE, TFIIH, or NCOA3). Interestingly, by GO analyses, each class was enriched with different biological gene sets (Fig. 8; Supplementary information, Fig. S6k, n, and Table S1). It should be emphasized that the largest class contained genes that were not rescued by ERRβ derivatives with mutations that individually compromised interactions with ERREs, TFIIH, and NCOA3 (Class 1 in Fig. 8d). These results, together with CFAs, which demonstrated that individual ERRβ mutants do not restore the self-renewal ability of ERRβ-KO ESCs (Fig. 7b), underscore a requirement for all interactions for the ERR transactivation function and support the general model from the biochemical studies. On the other hand, a subset of genes was not reliant on one or two of the analyzed interactions (Classes 2–7 in Fig. 8d), indicating that all three kinds of interactions are not always required and are redundant for target gene activation. Moreover, other subsets of target genes were successfully rescued by individual DNA-, TFIIH-, and NCOA3-binding mutants of ERRβ (Class 8 in Fig. 8d).

Although the underlying basis for what determines pathway choice for each class remains unclear, enriched motif analysis at ERRβ-binding sites proximal to target genes indicated several potential mechanisms. First, 1–3 bp sequences adjacent to core ERREs were found to vary between classes (Supplementary information, Fig. S6n). In light of NR structural studies that show how different recognition sequences confer different NR conformations and cofactor dependencies,[65–67] one possibility is that the ERRβ interactions with ERREs containing class-specific adjacent sequences might affect ERRβ conformation to facilitate preferential binding with one or the other factor (e.g., TFIIH vs. NCOA3). Alternatively, because binding motifs for various transcription factors, including pluripotency-related activators, were differentially enriched in each class (Supplementary information, Fig. S6n), these colocalizing activators might substitute for ERRβ and interact with their preferred factor. Indeed, specific genomic sites in ESCs are reported to be targeted by multiple transcription factors, including ERRβ,[68–70] further raising the possibility that at some loci ERRβ might function just as an architectural factor to facilitate formation of multi-protein

regulatory complexes on target genes even without interacting with cognate ERRE, TFIIH, or NCOA3 (Class 8 in Fig. 8d). Future studies will be directed at understanding how these variables control ERR–cofactor interactions. Furthermore, it remains unclear whether the observed ERRβ-mediated repression of genes regulating RNA-related cellular function reflects direct effects — our in vitro studies revealed evidence only of transcription activation — this possibility is consistent with previously reported interactions of ERRβ with transcriptional repressors and corepressors.[71,72]

Distinct and overlapping functions of ERR family members in ESCs

This study also highlights both redundancies and functional differences among ERR family members in ESCs, even as they behave indistinguishably in our current in vitro transcription assays that are mainly designed to reveal critical cofactor dependencies under specified constraints. It was previously shown that ERRα and ERRγ targeted a common set of promoters and interacted with a similar set of proteins.[73,74] Nonetheless, we found that ERRγ, but not ERRα, could replace ERRβ for ESC self-renewal; indeed, ERRβ and ERRγ regulated almost the same set of genes (Fig. 8a). Moreover, and most importantly, our biochemical analyses showed AF2-dependent interactions of ERRβ and ERRγ, but not ERRα, with NCOA3. Thus, because it mimics an ERR mutant defective in interaction with NCOA3, ERRα is unable to substitute for ERRβ in ESCs. While not ruling out interactions with additional AF2-binding cofactors in ESCs, these results simultaneously confirm the reported requirement of NCOA3 and establish a basis for the selective function of ERRβ (and ERRγ) in these cells. These results also indicate that in ESCs, ERRβ and ERRγ may selectively interact with common coactivators besides TFIIH and NCOA3, possibly through their N-terminal AF1 regions that have relatively high homology (~60%) to each other but low homology (~20%) to ERRα.[9]

In summary, this study clearly shows that the AF2-binding cofactors PGC-1α and NCOA3, as well as GTF TFIIH, are direct interaction targets of ERR that are critical not only for gene activation in vitro but also for activation of specific sets of genes in ESCs that regulate their pluripotency. Future studies will be directed at teasing out the various constraints that dictate the various activation strategies uncovered here.

MATERIALS AND METHODS

Antibodies, reagents, and oligonucleotides

The detailed information for the antibodies, reagents, and oligonucleotides used in this study is summarized in Supplementary information, Table S4.

Plasmid construction

To construct plasmids that included the full-length, deleted, or point mutated coding regions of each gene, DNA fragments with appropriate restriction enzyme sites at both ends were amplified from mouse and human cDNAs by conventional PCR methods,[75] and then introduced into each plasmid. The detailed information of restriction enzyme sites, tag sequences, linker sequences, and cDNA for each construction are summarized in Supplementary information, Tables S5 and S6. To express FLAG-tagged human (h) and murine (m) proteins (F-hERRα, F-hERRβ-L, F-hERRβ-S, F-hERRγ-L, F-hERRγ-S, F-mERRα, F-mERRβ, F-mERRγ-L, F-mERRγ-S, F-h/mERRs-DBDm point mutants, F-h/mERRs-AF2M point mutants, F-hERRα deletion mutants, F-hPGC-1α, F-hPGC-1α-mL point mutants, F-hPGC-1α-N deletion mutants, F-hPGC-1α-C deletion mutants, F-hNCOA1, F-hNCOA2, F-hNCOA3), StreptagII-His-tagged proteins (SH-hERRα, SH-hERRα-DBDm point mutants, SH-hERRα-AF2 point mutants, SH-hERRα deletion mutants), and GST-tagged proteins (GST-hERRs, GST-hERRα deletion mutants, GST-PGC-1α WT and mutants) in insect cells, open reading frame (ORF) with tag sequence(s) was introduced into *Nde*I site-disrupted pVL1392 baculovirus transfer vector[75] (BD Bioscience) to construct pVL1392-F, -SH, and -GST vector, respectively. For expression of only the GST-tag for control experiment, a stop codon was introduced instead of cDNA sequence. To express NCOA3 in insect cells, FLAG and His tags were introduced at the N- and C-termini, respectively. The NCOA3 ORF containing the appropriate tag sequences was introduced into the pFastBac1 baculovirus transfer vector (Thermo Fisher Scientific) to construct the pFB1-F-NCOA3-His vector. To express FLAG-tagged proteins (F-TFIIH core complex components,[76] F-Luciferase, and F-hERRα-DBDm) and His-TEV-tagged protein (HT-hERRα WT and mutants) in *Escherichia coli*, each ORF with tag sequence(s) was introduced into pET11d vector (Novagen) to prepare pET-F and pET-HT plasmid, respectively. For ectopic expression of human ERRα and PGC-1α in MEFs, AdEasy adenovirus expression system was used.[77] StreptagII-His-tagged human ERRα ORF and FLAG-tagged human PGC-1α ORF (full-length, or ΔC5) were introduced into pAdTrack-CMV vector to generate pAdTrack-CMV-SH-hERRα and pAdTrack-CMV-F-hPGC-1α, respectively. For ectopic expression of ERRs in ESCs, FLAG-tagged mouse ERRs and their mutants were introduced into the lentiviral vector pAiLV[78] to generate pAiLN-F-mERRs. To generate a template for ERR-dependent in vitro transcription, three tandem copies of the *ACADM* ERRE were introduced between *Eco*RI and blunted *Pst*I sites of the G-free cassette carrying pG5HMC2AT[79] to generate pERRE3HMC2AT. For luciferase assay, a pERRE3HMC2AT fragment released by digestion of the *Hind*III site upstream of ERRE sequences (see Supplementary information, Table S5) and the downstream *Xho*I site in the G-free region was introduced between the *Hind*III and *Xho*I sites of pGL3-basic (Promega) to generate pGL3-ERRE3HMC2AT as a reporter plasmid. For effector plasmids, ORF of proteins of interest (hERRα, hERRα-ΔAF2, PGC-1α) with three tandem FLAG sequences were introduced into pcDNA3.1(–) (Invitrogen). For MED1 knockdown in MEFs, pLKO1 vectors having shRNA against mouse MED1 (Sigma, Cat# SHCLNG-NM_013634, clone ID: TRCN0000099578) and control scrambled shRNA vector were used. The original puromycin resistance gene in pLKO1 was replaced with a blasticidin resistance gene. For PPARγ/RXRα-dependent in vitro transcription, a previously described template[20] was used. The plasmid vector for GST-TFIIB was used as described.[80] The plasmid vector for F-p53 was used as described,[81] as were the vectors for F-mPPARγ and F-hRXRα.[20]

Cell culture conditions

Sf9 and High Five insect cells were maintained in Grace's medium (Gibco) with 10% FBS, 50 μg/mL gentamycin (Gibco), and 1× Pluronic F-68 (Gibco) on plates or in spinner flasks at 28 °C. MEFs, MED1-KO MEFs,[82] 293T, HEK293 cells were maintained in high-glucose DMEM (Gibco) with 10% FBS and 1% penicillin-streptomycin (Sigma) at 37 °C with 5% CO_2. Trypsin (Sigma) was used to transfer cells.

ESC line K3 derived from C57BL6NCrSlc/129 hybrid blastocysts[83] was maintained on gelatin (Sigma)-coated plates with GMEM (Sigma) supplemented with 10% ES cell-qualified FBS (Gibco), 0.1 mM 2-mercaptoethanol (Gibco), 1× non-essential amino acids (Gibco), 2 mM L-glutamine (Gibco), 1 mM sodium pyruvate (Gibco), 1% Penicillin-Streptomycin (Sigma), 1 μM PD0325901 (BioVision), 3 μM CHIR99021 (BioVision), and 1000 unit/mL LIF (Millipore) or in N2B27 medium including PD0325901, CHIR99021, and LIF (PD/CH/LIF), or sometimes without LIF (PD/CH) as indicated in the text. N2B27 medium is composed of a mixture of DMEM/F12 medium (Gibco) and Neurobasal medium at a ratio of 1:1, containing 0.1 mM 2-mercaptoethanol, 1× non-essential amino acids, 1% GlutaMAX supplement (Gibco), 1% Penicillin-Streptomycin (Sigma), 1× N-2 supplement (Gibco), and 1× B-27 supplement (Gibco). TripLE express (Gibco) was used to detach ESCs cultured in N2B27; cells were extensively washed twice with DMEM/F12 (Gibco) including 0.1% BSA before seeding to the next plate. ESCs cultured in GMEM were detached with standard trypsin (Sigma). These culture conditions were essentially as described elsewhere.[83–85]

Bacterial strains

For protein expression, Rosetta(DE3)pLysS (Novagen) was transformed with the appropriate pET vector (Novagen) and cultured in LB broth (Sigma) supplemented with 100 μg/mL ampicillin (Sigma) and 40 μg/mL chloramphenicol (Sigma). For pAdEasy plasmid preparation for adenovirus generation, the AdEasier (Stratagene) strain was transformed with pAdTrack vector (see below) by electroporation (2-mm cuvette, pulse at 2500 V, 200 Ω and 25 μF) and cultured in LB broth (Sigma) supplemented with 25 μg/mL kanamycin.

Protein preparations

Recombinant TFIIA, TFIIB, TFIIE, TFIIF, TFIIH, and PC4 were newly prepared as described.[75] TFIID, RNA polymerase II, WT Mediator complex, and MED1-

lacking Mediator complex were newly purified as described.[21,36] Recombinant TFIIS was newly prepared as described.[86] Recombinant histones, NAP1, ACF/ISWI, p300, and TopoI were prepared as described.[87] PCAF was newly purified as described.[88]

Protein purifications described below were carried out in our standard "BC" buffer system. Its basic composition is 20 mM HEPES-KOH (pH 7.9 at 4 °C), 1 mM EDTA, 10% glycerol, 0.5 mM PMSF, and varying concentrations of KCl, which are specified (e.g., BC100 for buffer containing 100 mM KCl). If the KCl is replaced with NaCl, it is noted (e.g., BC100-NaCl). Further additions are also specified. These include: NP (% NP40); TR (% Triton X-100); D (mM DTT); PI (protease inhibitor for mammalian cells (Sigma), 1/200 (v/v) dilution when added); MG (MG132 (Sigma), 5 μM, when added). Thus, for example, BC100-NaCl-NP0.1D1PIMG indicates that the BC-buffer contains 100 mM NaCl, 0.1% NP40, 1 mM DTT, 1/200 protease inhibitor, and 5 μM MG132.

Typically, baculoviruses expressing FLAG-, GST-, and SH-tagged proteins were prepared by baculogold baculovirus expression system (BD Bioscience) with pVL1392-F, pVL1392-GST, and pVL1392-SH transfer vectors, respectively (see above), as described previously.[75] Baculovirus expressing F-NCOA3-His was prepared by Bac-to-Bac expression system (Thermo Fisher Scientific) with pFB1-F-NCOA3-His transfer vector according to the manufacturer's instructions. High Five cells were infected with the resulting baculovirus for 2 days to express recombinant proteins.

Recombinant FLAG-tagged human and mouse ERRs (F-hERRα, F-hERRβ-L, F-hERRβ-S, F-hERRγ-L, F-hERRγ-S, F-mERRα, F-mERRβ, F-mERRγ-L, and F-mERRγ-S), and their various mutants (F-h/mERRs-DBDm point mutants, F-h/mERRs-AF2M point mutants, F-hERRα deletion mutants) were expressed in High Five cells, harvested, and then sonicated in BC100-NaCl-D1PIMG. After ultracentrifugation, the soluble fraction was subjected to a HiTrap-Q column (Cytiva). The bound proteins were eluted by a linear gradient from BC100-NaCl-D1 to BC1500-NaCl-D1. F-ERR-containing fractions eluted from BC225-NaCl to BC275-NaCl were pooled and the salt concentration of the pooled fractions was adjusted to BC100-NaCl-D0.1. The protein was next subjected to HiTrap-Heparin column (Cytiva), and the bound proteins were eluted by a linear gradient from BC100-NaCl-D0.25 to BC1500-NaCl-D0.25. The F-ERR-including fractions eluted from BC525-NaCl to BC575-NaCl were pooled, and the salt concentration of pooled fractions was adjusted to BC500-NaCl-NP0.1D0.25. Affinity chromatography on M2-agarose (Sigma) was then carried out. M2-agarose was extensively washed with BC500-NaCl-NP0.1D0.25, and the bound proteins were eluted with BC500-NaCl-NP0.1D0.25 containing 0.15 mg/mL 3× FLAG peptide (Sigma). Although elution profiles of WT and point mutant F-ERRs from HiTrap-Q and HITrap-Heparin columns were exactly the same as described above, F-hERRα deletion mutants were eluted from HiTrap-Q and HiTrap-Heparin columns by lower salt concentration than the WT, and F-hERRα-AF1 was recovered in the flow-through fraction from HiTrap-Heparin column.

Recombinant FLAG-tagged human PGC-1α (F-hPGC-1α) and its various mutants (F-hPGC-1α-mL points mutants, F-hPGC-1α-N deletion mutants, F-hPGC-1α-C deletion mutants) were expressed in High Five cells. Extracts were prepared by Dounce homogenization, first of the harvested cells in BC0-D1PIMG and then of the resulting nuclear pellets in BC500-D1PIMG. Both fractions (cytoplasmic and nuclear) were centrifuged and the supernatants were mixed together. The salt concentration of the pooled extract was adjusted to BC100-D1, and then ultracentrifuged again. This final supernatant was subjected to HiTrap-Heparin column. Bound proteins were eluted by a linear gradient from BC100-D0.25 to BC1000-D0.25. The F-PGC-1α-containing fractions eluted from BC200 to BC250 were pooled, and the salt concentration of the pooled fractions was adjusted to BC300-NP0.1D0.25. This fraction was further purified on M2-agarose in BC300-NP0.1D0.25. All point mutants and deletion mutants were purified by the same methods used for WT F-hPGC-1α as above, but slight differences with respect to the salt concentration at which each deletion mutant eluted from the HiTrap-Heparin column were evident. Notably, ΔC2 and ΔC3 were recovered in the flow-through fractions.

Recombinant FLAG-tagged mouse PPARγ2 (F-mPPARγ2) and human RXRα (F-hRXRα) were prepared with the baculovirus expression system as described[20] and the proteins were purified by a protocol similar to that used for F-hPGC-1α purification. Briefly, the extract prepared by sonication in BC100-D1PIMG was subjected to HiTrap-Q column followed by M2-agarose purification. The fractions were eluted from HiTrap-Q column by a linear gradient with F-mPPARγ2 eluted between BC250-D0.25 and BC300-D0.25 and F-hRXRα eluted between BC150-D0.25 and BC200-D0.25.

Recombinant FLAG-tagged human NCOA1, NCOA2, and NCOA3 (F-hNCOAs) were expressed in High Five cells and clear supernatants were prepared as for F-hPGC-1α. The supernatant was adjusted to BC300-NP0.1D0.25 and then F-NCOAs were directly purified by M2-agarose (Cytiva) as F-hPGC-1α. Recombinant FLAG-NCOA3-His was similarly expressed in High Five cells. Whole cell lysate was prepared in BC500-NP0.1PIMG (EDTA–) and used for pull-down assay.

Recombinant GST, GST-ERRs (GST-hERRα, GST-hERRβ-L, GST-hERRβ-S, GST-hERRγ-L, GST-hERRγ-S) and GST-hPGC-1α (full-length and its deletion mutants ΔN1–ΔN9 and ΔC2–ΔC10) were expressed in High Five cells as FLAG-tagged proteins. Whole cell lysates were prepared in BC100-TR0.1D1 by sonication. The cleared lysates after centrifugation were directly used to prepare GST protein-bound Glutathione Sepharose beads (Cytiva) for GST pull-down assay (see below).

Recombinant TFIIH core and CAK subcomplex were reconstituted via a baculoviral expression system essentially as described.[76] Modifications included use of only baculoviruses II and III, and baculovirus I to infect High Five cells for expression of TFIIH core and CAK subcomplex, respectively. After the infection, cells were harvested and sonicated in BC500-PIMG (EDTA–) for TFIIH core and in BC500-TR0.1PIMG for CAK. The post-ultracentrifugation cleared lysate containing TFIIH core subunits was first purified by TALON resin (Clontech) as described for Ni-NTA-agarose purification of holo-TFIIH.[76] The corresponding lysate containing the CAK subcomplex was first purified by M2-agarose in BC500-TR0.1D0.25. The purified fractions were then subjected to Superdex200 10/300 GL gel filtration column (Cytiva) in BC500-D1 and peak fractions were pooled.

TFIIH core subunits (F-XPB, F-XPD, F-p62, F-p52, F-p44, or F-p34) were expressed in Rosetta(DE3)pLysS (Novagen) transformed with pET-F vectors expressing the individual subunits. Log phase cells were induced with 1 mM IPTG and allowed to express the recombinant proteins at room temperature (RT) for 3 h. The whole cell lysate was prepared by sonication in BC300-NP0.1D0.25. The supernatant after ultracentrifugation was mixed with M2-agarose and purified as for F-hPGC-1α. For the ITA performed under stringent conditions (Fig. 5h), F-p52 was further purified by Superdex200 10/300 GL column with BC300-D1 and fractions containing F-p52 were pooled for the assay.

Recombinant GST-TFIIB was expressed in Rosetta(DE3)pLysS (Novagen) as described above for the TFIIH subunits. Cleared lysate was prepared as for GST proteins expressed in High Five cells and used directly for the assay.

Recombinant FLAG-tagged luciferase and FLAG-tagged p53 were expressed in bacteria as described for TFIIH core subunits. Cleared lysates were prepared in BC100-D1 and subjected to HiTrap-Heparin column. The F-luciferase in flow-through faction was used directly in binding assays (see below). For F-p53, HiTrap-Heparin-bound proteins were eluted by a linear gradient from BC100-D0.25 to BC1000-D0.25. The fractions around 400 mM KCl that contained F-p53 were pooled and used for binding assays (see below).

Details of the purification procedures for the individual proteins are also summarized in Supplementary informaiton, Table S7.

Gel shift assay

Double-stranded DNA probes containing ACADM-ERRE were prepared by annealing oligonucleotides (see Supplementary information, Table S4) and labeled with ^{32}P-γ-ATP (Perkin Elmer) by filling protruding DNA ends with Klenow fragment (NEB). The probe was separated by 5% polyacrylamide gel electrophoresis, extracted from the probe-containing gel by smashing and vortexing, and concentrated by Amicon ultra-4 centrifugal filter unit with a membrane NMWL of 10 kDa (Millipore). The probe (20000 cpm) was added to gel shift buffer containing 40 mM HEPES-KOH (pH 7.9), 60 mM KCl, 8 mM $MgCl_2$, 5 mM DTT, 20 μg/mg poly (dI-dC) (Sigma), and 0.025% NP40, and 30 ng F-hERRα. The reaction was incubated at 30 °C for 30 min and analyzed by 5% polyacrylamide gel with 0.5× TBE buffer. The gel was dried and autoradiographed by exposing to a sheet of X-ray film.

In vitro transcription

In vitro transcription from DNA templates (pERRE3HMC2AT) was performed as described[75] with some modifications. Briefly, 25 ng pERRE3HMC2AT was first mixed with 15 ng F-ERRs and incubated at 30 °C for 30 min. These components were mixed with GTFs (10 ng TFIIA, 5 ng TFIIB, 150 ng TFIID, 5 ng TFIIE, 10 ng TFIIF, 75 ng TFIIH), 300 ng RNA polymerase II, 200 ng Mediator, 200 ng PC4, and the reaction mixture (1 μL (10 μCi) ^{32}P-α-CTP (Perkin Elmer), 5 nmol ATP/UTP (Cytiva), 0.313 nmol CTP (Cytiva), 2.5 μmol 3′-O-metyl-GTP (TriLink), 0.2 μmol $MgCl_2$, 125 nmol DTT, 1 mmol HEPES-KOH (pH 7.9, at 4 °C), 10 units RNasin plus (Promega) in a total volume of 25 μL (Fig. 1a). Thirty nanograms of F-hPGC-1α was added

to the reaction at this step if specified. For the competition assay, the template was first mixed with ERRα and then supplemented with F-p52. The reaction was incubated at 30 °C for 30 min, and finally mixed with GTFs, cofactors, polymerase, and reaction mixture.

For in vitro chromatin transcription, chromatin was assembled on pERRE3HMC2AT as described.[87] Briefly, 260 ng H2A/B, 310 ng H3/H4, 6 µg NAP1, 20 µg BSA (Roche) were mixed together in total 60 µL HEGK buffer containing 100 mM KCl. After 15 min on ice, 300 ng template DNA, 212 nmol ATP (Cytiva), 1.5 µg creatine phosphokinase (Sigma), 2.12 µmol creatine phosphate (Sigma), 0.3 µmol $MgCl_2$, 5 ng Topo1, and 150 ng dACF/ISWI were added in a total volume of 100 µL. After 2-h incubation, the chromatin template was used for MNase assay[89] or transcription reaction. Chromatin transcription reactions were performed stepwise, as summarized in Fig. 1d. Briefly, the chromatin template (30 ng pERRE3HMC2AT per reaction) was first combined with 36 ng F-ERRs, and incubated at 30 °C for 15 min. To the reaction, 26 ng p300, 1 µL of 0.5 mM acetyl CoA (Sigma), and 30 ng PGC-1α were added, followed by incubation at 30 °C for 15 min. Next, twice the amount of GTFs (TFIIA, TFIIB, TFIID, TFIIE, TFIIF, TFIIH), RNA polymerase II, and cofactors (Mediator and PC4) used in DNA-templated transcription reactions was added. When HeLa cell nuclear extract[75] was included, 40 µg was added at this step. After 15 min incubation at 30 °C for 15 min, the reaction was finally mixed with 75 ng TFIIS and a transcription reaction mixture containing nucleotides and other additives was added to a total volume of 50 µL, as described for naked DNA transcription.

For both DNA-templated and chromatin transcription, all factors were diluted in BC100 containing 0.2 mg/mL BSA (Roche). Moreover, the final salt concentration of reactions across an experiment was strictly maintained at 60 mM KCl. The salt concentrations of all reactions at each step were also adjusted even when factors were added to a subset of the reactions using, if necessary, BC100 containing 0.2 mg/mL BSA.

After the 45 min transcription step, reactions were first treated with 2 units of DNaseI (NEB) and 15 units of RNaseT1 (Thermo Fisher Scientific) at 37 °C for 30 min and then with 10 µg Proteinase K (Sigma) in 200 µL STOP buffer (10 mM EDTA, pH 8.0, 0.2% SDS, 0.4 mg/mL tRNA (Sigma)) at 37 °C for 30 min. The reactions were extracted with phenol/chloroform, ethanol-precipitated, and dissolved in formamide at 98 °C for 3 min. The transcripts were separated by 5% polyacrylamide/8M urea/1× TBE gel and subjected to autoradiography against a sheet of X-ray film or phosphorimaging against storage phosphor screen for the Storm or Typhoon systems (Amersham) to measure the band intensity.

In vitro chromatin transcription with 3DR1 template[20] and PPARγ/RXRα was performed by the same protocol as for ERRα, in the presence of 15d-PGJ2.

ITAs

ITAs were performed as described previously[19] with modifications to ensure sequential additions of factors. For ITAs with ERRα, a biotinylated ERRE3-HMC2AT fragment was amplified from the pERRE3-HMC2AT in vitro transcription template by PCR with a biotinylated M13R and M13F primer set, purified, and immobilized on Dynabeads M280 streptavidin. Two and half microliters of the beads immobilized with 100 ng template DNA were incubated with 100 µL of the blocking buffer (50 mM Tris-HCl, pH 7.9 at 4 °C, 100 mM KCl, 0.01% NP40, 10 mM DTT, 0.5 mM PMSF, single strand salmon sperm DNA (Thermo Fisher Scientific), poly(dI-dC) (Sigma), BSA; see below for the concentration of DNA and BSA) at 30 °C for 15 min. For the sequential addition of factors, the first purified protein in wash buffer (50 mM Tris-HCl, pH 7.9 at 4 °C, 100 mM KCl, 0.01% NP40, 0.5 mM DTT, 0.5 mM PMSF) was initially mixed with the beads. After incubating at 30 °C for 30 min with continuous rotation, the beads were washed three times at RT with 400 µL wash buffer (each wash was 3 min with rotation). Subsequent blocking/binding/washing steps were carried out sequentially as specified. The concentrations of carrier DNA and BSA in the blocking buffer were optimized for each factor. Thus, ERRs (100 ng): 2 ng/µL DNA, 0.05 mg/mL BSA; PGC-1α (2.2 pmol): 0.5 ng/µL DNA, 0.2 mg/mL BSA; Mediator (200 ng): 10 ng/µL DNA, 0.2 mg/mL BSA; p300 (100 ng): 2 ng/µL DNA, 0.2 mg/mL BSA; and TFIIH core subunits (3.1 pmol): 2 ng/µL DNA, 0.2 mg/mL BSA. For proteins diluted in wash buffer, final KCl and NP40 concentrations were carefully adjusted to 100 mM and 0.01%, respectively. The template-bound proteins were finally eluted in 30 µL of SDS-PAGE sample buffer and subjected to SDS-PAGE followed by immunoblotting with specific antibodies to detect proteins as indicated in the figures. For ITA with PPARγ/RXRα, the template was amplified from the p3DR1 plasmid[20] and ITA was performed as described for ERRα, in the presence of 15d-PGJ2. For ITA with ERRβ/γS, NCOA3, and Mediator, DNA-bound beads were first mixed with ERRβ/γS, washed, and then mixed with NCOA3 and Mediator simultaneously using the same carrier DNA concentration as described for PGC-1α. For ITA experiments in which crude extracts containing F-hERRα and its mutants were used, the proteins were expressed in bacteria, sonicated in wash buffer, and the post-ultracentrifugation cleared lysates were directly added to the DNA-bound beads without any carrier DNA.

Because p52-binding deficiency of ERRα-DBD mutants was not clearly detected under standard conditions, more stringent conditions were used to analyze p52 binding to ERRα mutants (Fig. 6h) as described,[39] with some modifications of buffer compositions. Template preparation, sequential addition of factors, washing, and analysis of bound fractions were identical to the standard ITA above. For blocking, 100 µL of assay buffer (20 mM HEPES-KOH, pH 7.9, 4 mM $MgCl_2$) containing 5 mg/mL BSA, 12.5 mM DTT, 2 mg/mL polyvinylpyrrolidone, and 0.03% NP40 was used. Four hundred nanograms of F-hERRα (WT and DBD mutants) and 120 ng F-p52 was diluted in 50 µL of assay buffer containing 0.45 mg/mL BSA, 1.25 mM DTT, and 35 ng/mL sonicated *E. coli* DNA. Two types of wash buffers were used: one was composed of 20 mM HEPES, pH 7.9, 60 mM KCl, 4 mM DTT, 4 mM $MgCl_2$, and 0.01 % NP40, which was used for the washing step after ERRα binding. For the buffer used after p52 had been added, KCl and NP40 concentrations were increased to 100 mM and 0.1%, respectively. Finally, the beads were boiled with SDS-PAGE sample buffer and proteins were detected by immunoblotting with specific antibodies as indicated in the figures.

Pull-down assays

GST pull-down assays were performed as described.[75] Typically, 10 pmol GST-tagged proteins were bound to Glutathione-Sepharose beads by mixing the beads with an appropriate volume of cleared cell lysates containing the GST-tagged proteins (see above for lysate preparation). After binding of GST-tagged proteins to the beads at 4 °C for 1 h, the beads were washed with BC100-TR0.1D1, mixed with 40 pmol recombinant proteins or ~5 pmol of a given purified complex in BC100-TR0.1D1 containing 0.4 mg/mL BSA, and incubated at 30 °C for 2 h. After washing with BC100-TR0.1D1, and elution by boiling in SDS-PAGE sample buffer, the samples (and input proteins) were analyzed by SDS-PAGE and immunoblotting with specific antibodies.

Pull-down assay with F-NCOA3-His was performed with 10 pmol of F-NCOA3-His immobilized by directly mixing cleared whole cell lysate with TALON resin (Clontech). After extensive washing of the beads, first with BC500-NP0.1 and then BC100-NP0.1, the beads were mixed with 3 µg of Mediator, incubated, washed with BC100-NP0.1, and eluted by boiling in SDS-PAGE sample buffer. The samples (and input proteins) were analyzed by SDS-PAGE and immunoblotting with specific antibodies.

Immunoprecipitation binding assays

Excess amounts of FLAG-tagged proteins (F-hERRα, F-p53, or F-luciferase) in relevant chromatographic fractions (F-luciferase, HiTrap-Q; F-hERRα and F-p53, HiTrap-Heparin) were incubated with 5 µL M2-agarose in BC300-NP0.1D0.25 for 2 h at 4 °C. After extensive washing with BC300-NP0.1D0.25, 1 µg PC4 was added to the beads in the same buffer. After a 2-h incubation at 4 °C, the beads were washed with BC300-NP0.1D0.25 and eluted by boiling in 50 µL SDS-PAGE sample buffer. The samples were then subjected to SDS-PAGE followed by immunoblotting with PC4 antibody.

Dimerization assay

For the hERRα dimerization assay, High Five cells were co-infected with baculoviruses expressing FLAG-tagged and SH-tagged hERRα derivatives (WT, ΔAF2, ΔLBD, AF2M6, or DBD mutants), cultured for 2 days, and harvested. The cell pellets were resuspended in BC100-NP0.01D0.25PIMG and sonicated by Bioruptor UCD-200 (Diagenode). The cleared lysates were directly mixed with M2-agarose. After incubation at 4 °C for 1 h, the beads were washed with BC100-NP0.1D0.25 five times and eluted by boiling in SDS-PAGE sample buffer. The eluted fractions, together with the input lysates, were analyzed by SDS-PAGE followed by immunoblotting with specific antibodies as indicated in the figures.

In vitro modification assays

In vitro phosphorylation of F-hERRα (WT, ΔAF2, ΔLBD, ΔHinge, and ΔDBD) or HT-hERRα (WT and S19/22A) by TFIIH was performed as described[90] with minor modifications. Recombinant proteins (15 pmol) were mixed with

100 ng recombinant TFIIH in 15 µL H1 kinase buffer containing 100 mM KCl. The reactions were incubated at 30 °C for 30 min and analyzed by SDS-PAGE followed by CBB staining, and autoradiography on X-ray film.

To analyze phosphorylation of F-ERRs and other proteins by PKA and PKCδ, 15 pmol of each recombinant protein (histone H3/H4, luciferase, F-hERRα (WT, ΔAF2, ΔLBD, ΔHinge, ΔDBD, and DBDm3, DBDm6, DBDm19, AF2M6)) was mixed with 50 ng recombinant PKA (Millipore) or 25 ng recombinant PKCδ (Millipore) in the buffer recommended by the manufacturer, and analyzed as in the case of TFIIH.

In vitro acetylation of F-hERRα and other proteins by PCAF was performed as described[91] with 15 pmol of each recombinant protein (histone H3/H4, luciferase, F-hERRα (WT, ΔAF2, ΔLBD, ΔHinge, ΔDBD, and DBDm3, DBDm6, DBDm19, AF2M6)) and purified PCAF,[88] and analyzed as for the phosphorylation assay. The gel was treated with Amplify fluorographic reagent (Cytiva) to increase detection efficiency.

Luciferase assays

Luciferase assays were performed as described[75] with minor modifications. Briefly, 3×10^5 293T cells were seeded onto 48-well plates, cultured for one day, and transfected with 22 ng pGL3-ERRE3HMC2AT, 0.1 ng pRL-SV (Promega), 70 ng pcDNA3.1–3× FLAG-hPGC-1α, and 70 ng pcDNA3.1–3× F-hERRα (full-length or ΔAF2) by using TransIT-LT1 transfection reagents (Mirus) according to the manufacturer's instructions. After 24 h, reporter luciferase gene expression was measured by using Dual-Luciferase Reporter Assay System (Promega) and firefly luciferase activities were normalized against Renilla luciferase controls.

Virus preparation

Adenoviruses expressing SH-tagged human ERRα and FLAG-tagged human PGC-1α (full-length and ΔC5 mutant) were prepared by using adenovirus plasmid pAdEasy-CMV-SH-hERRα and pAdEasy-CMV-FLAG-mPGC-1α as described.[77] Briefly, HEK293 cells were transfected with *Pac*I-linearized pAdEasy adenovirus plasmid by Trans-IT LT1 (Mirus), harvested, lysed by freezing and thawing, and amplified 3–5 times until sufficient titer was obtained.

Lentiviruses expressing FLAG-tagged mouse ERRs, rtTA, and GFP were prepared by using the pAiLN-F-mERRs plasmid. pAiLN-F-mERRs plasmids were transfected into 293T cells with pMDLg/pRRE and pCMV-VSVG-RSV/Rev at a ratio of 2:1:1, with TransIT-LT1 transfection reagent (Mirus) according to the manufacturer's instructions. The medium was changed 18 h after transfection, and the virus-containing medium was harvested twice after one-day incubation periods. The pooled virus suspension was concentrated by centrifugation at 8000 rpm for 16 h for efficient infection.

To prepare lentivirus for knockdown of MED1, pLKO1 vectors expressing shRNA for MED1 (see above) were transfected into 293T cells with psPAX2 and pMD2.G at a ratio of 10:9:1, usingTransIT-LT1 transfection regent (Mirus) according to the manufacturer's instructions. The medium was changed 18 h after transfection, and the virus-containing medium was harvested twice after one-day incubation periods. The medium was used directly for MED1 knockdown in MEFs.

MED1 knockdown in MEFs

MEFs were infected with lentivirus expressing shRNA for MED1 or scrambled shRNA (see above) in the presence of 8 µg/mL Polybrene. Fresh medium was added 1 day after infection. After incubation for 1 day, the cells were selected with 10 µg/mL blasticidin (Invitrogen). MED1 knockdown in bulk-expanded blasticidin-resistant cells was analyzed by SDS-PAGE followed by immunoblotting with anti-MED1 antibody (Bethyl Laboratories Inc.).

ERRα- and PGC-1α-expressing MEFs, RT-qPCR, and ChIP

MEFs, MED1-KO MEFs, and MED1-knockdown MEFs (see above) were infected with adenovirus expressing SH-hERRα and either WT or ΔC5 F-hPGC-1α. Two days after the infection, the cells were used for target gene analysis. RNA was extracted from these cells using an RNeasy kit (Qiagen) with a DNaseI treatment step, and corresponding cDNA was synthesized by Superscript III kit (Invitrogen). Expression of *cycs* and *idh3a* genes was analyzed by RT-qPCR of the synthesized cDNA in a Quantitect SYBR Green PCR master mix (Qiagen) with appropriate primer sets (Supplementary information, Table S4). Fold-changes of each gene expression were calculated by the $2^{\Delta Ct}$ method.

For ChIP assay, typically 1.5×10^6 cells were seeded on a 150 mm plate, infected with adenovirus(es) 12 h after seeding, and then cultured for 1.5 days. ChIP procedure was performed as described[92] with slight modifications. Briefly, the cells were fixed in fresh non-supplemented DMEM containing 1% methanol-free formaldehyde (Thermo Fisher Scientific) at RT for 10 min. The reaction was quenched with 0.125 M glycine at RT for 5 min. The cells were washed twice with ice-cold PBS (–) on the plate, and collected by a scraper with PBS (–) containing 0.5 mM PMSF and 0.01% Triton X-100. After centrifugation at 1000 rpm for 10 min, the cell pellets were washed twice with PBS (–) containing 0.5 mM PMSF and 0.01% Triton X-100 in a microtube. The cell pellets were suspended in 100 µL/plate of RIPA-0 buffer containing 0.25% Sarkosyl (Sigma), 1/200 volume of a protease inhibitor cocktail for mammalian cells (Sigma), and 0.5 mM PMSF. Fragmentation of chromatin was performed by sonication with S220 (Covaris) to an average chromatin length of ~500 bp. Small aliquots of chromatin lysate were first treated with RNaseA (Qiagen), de-crosslinked, and treated with Proteinase K (Sigma), as described for the eluates (see below), to determine the DNA concentration in the original lysate. Lysates containing the same amounts of genomic DNA were used for each immunoprecipitation. Typically, lysates containing 15–30 µg DNA, which roughly corresponded to two 150 mm plates, were used for one immunoprecipitation with a given antibody. The lysate was brought to a final NaCl concentration to 0.3 M, and mixed with 10 µL Dynabeads Protein A (Thermo Fisher Scientific) pre-bound with 2 µg of the antibody. After incubation at 4 °C overnight, the beads were sequentially washed with RIPA-0.3 buffer three times, RIPA-0 buffer twice, LiCl buffer twice, and finally twice with TE containing 0.01% NP40. The precipitated chromatin was eluted twice with 100 µL of TE containing 1% SDS at 65 °C for 30 min. The eluted chromatin was de-crosslinked overnight at 65 °C in the presence of 0.2 M NaCl. The overnight reaction also included 10 µg/mL RNaseA (Qiagen). The eluate was further treated with 0.1 µg/mL Proteinase K (Sigma) at 55 °C for 2 h. Finally, the DNA was purified on Qiaquick PCR purification columns (Qiagen). RT-qPCR was performed with this product using the PowerUp SYBR Green master mix (Thermo Fisher Scientific), and appropriate primer sets (Supplementary information, Table S4). Finally, the amount of DNA fragment in each sample was calculated by the $2^{\Delta Ct}$ method and expressed in a graph as the average amount of the target amplicon in precipitates relative to input DNA.

Establishment of ERRβ-KO ESCs expressing F-ERRs

CRISPR/Cas9 technology was used to generate ERRβ KO in ESCs as described.[93] Briefly, ESCs were transfected with Cas9-expressing plasmid pX458 and a single guide RNA (Supplementary information, Fig. S6a). Cas9-expressing GFP-positive cells were single cell-sorted and expanded. The targeted region was amplified from genomic DNA purified with Wizard genomic DNA purification kit (Promega) by PCR with the primer set (Supplementary information, Table S4). PCR amplicons were subsequently cloned into a TA vector pGEMT-easy (Promega) and sequenced for genotyping. The ERRβ KO was also confirmed by analyzing a whole cell lysate prepared by directly resuspending 2×10^5 cells in SDS-PAGE sample buffer, followed by immunoblotting with an anti-ERRβ antibody (R&D systems).

To establish ERRβ-KO ESCs that inducibly express FLAG-tagged murine ERRs (F-mERRα, F-mERRβ, or F-ERRγ-S), ERRβ-KO cells were stably transduced with lentivirus prepared from pAiLV-F-mERR plasmids (see above), in the presence of 8 µg/mL Polybrene (Sigma). GFP-positive cells were single cell-sorted and expanded, and the expression of ectopic F-mERRs was checked in the presence of 2 µg/mL Dox (Sigma) by the protocol outlined in Supplementary information, Fig. S6c. These cells were designated KO/ERRβ-wt cells whereas ERRβ-KO ESCs that were transduced with a control lentivirus vector that does not express ERRβ were designated KO/mock cells.

CFA of ESCs and qPCR

For CFA, a 24-well plate was first coated with 400 µL of 0.01% poly-L-ornithine (Sigma; dissolved in water) at RT overnight. After washing with PBS (–) twice, it was coated with 310 µg/mL laminin (Invitrogen; dissolved in PBS (–)) at 37 °C overnight. After two washes with PBS (–), N2B27 medium was added to the plate. ESCs maintained in N2B27-LIF/PD/CH medium, with or without 2 µg/mL Dox, were seeded at the appropriate clonal density (200 cells/24-well plate). Medium contained either LIF/PD/CH or only PD/CH, with or without 2 µg/mL Dox. For RNA preparation, 1600 cells were seeded in a poly-L-ornithine- and laminin-coated 12-well plate in N2B27-LIF/PD/CH medium. After 4 days in culture, the cells were fixed in 4% paraformaldehyde and stained with alkaline phosphatase as described.[94] The stained colonies were scanned and quantified by using

Photoshop (Adobe) software as follows. The colonies were first automatically detected by the "color range" function against a fixed level of red color that covers all red colonies. This was followed by a manual correction to remove false positives, i.e., diffuse reflection from solution surface. Then paths against the selected pixels were made and the paths were filled with flat blue color, i.e., RGB code (0, 0, 255). The blue pixel was then automatically counted using the "counting tool" function against RGB (0, 0, 255) color and the counting log was recorded via the "record measurement" function. The colony number was finally calculated from total area value of the log. Note that we always used the same color extraction file for the "color range" function to detect red colonies so that the definition of red-colored colonies was statistically the same across the various assays.

To analyze pluripotency-related genes under 2i conditions, each ESC line was first seeded in N2B27-LIF/PD/CH medium and cultured for 12 h; after two rinses with a 1:1 mixture of DMEM/F12 and Neurobasal media, N2B27-PD/CH was finally added. After culturing for 3 days, the cells were harvested for RNA preparation using RNeasy (Qiagen) with inclusion of DNase treatment step. RT-qPCR was performed with Quantitect SYBR Green PCR master mix (Qiagen), appropriate primer sets (Supplementary information, Table S4), and cDNAs prepared from RNA purified using a SuperScript III kit (Invitrogen). Fold-changes of each gene expression were calculated by the $2^{\Delta Ct}$ method. Relative expression levels of ERRα/β/γ were determined by RT-qPCR with appropriate primer sets (Supplementary information, Table S4) and copy number-known plasmid vectors containing ERRα/β/γ cDNAs as standards.

RNA-seq and data analysis

RNA samples were obtained from two clones of each of WT/mock, KO/mock, KO/ERRβ-wt, KO/ERRβ-DBDm3, KO/ERRβ-DBDm6, KO/ERRβ-AF2M6, and KO/ERRβ (described in detail in the main text) ESC lines that had been cultured in N2B27-PD/CH medium and Dox for 3 days. The library for RNA-seq was prepared from 400–500 ng of isolated RNA by using TruSeq Stranded Total RNA with Ribo-Zero kit (Illumina) according to the manufacturer's instructions. The pooled libraries with unique index sequences were sequenced using NovaSeq SP (Illumina) with single-end 100 bp reads at the Rockefeller University Genomics Resource Center. The raw data and a count matrix (see below) are posted at Gene Expression Omnibus with accession number GSE196202.

To generate expression count matrix, raw reads were trimmed to remove adaptor sequences by Skewer (v.0.2.2) and mapped to mm10 genome by STAR (v.2.7.8a), and then mapped reads were counted by featureCounts (v.2.0.10).

The package of edgeR glmQLFTest (v3.32.1) was used to identify differentially expressed genes (DEGs) using the count matrix. Briefly, the library size normalization, the dispersion estimation, and then the generalized linear model fitting were sequentially performed with 'calcNormFactors(y, method = TMM), 'estimateDisp(y, design = design, robust = TRUE)', and 'glmQLFit(y, design = design)', respectively. Finally, $\log_2$ fold change (FC) and false discovery rate (FDR) of each gene between two groups were calculated by glmQLFTest. Genes with FDR < 0.05 and abs($\log_2$FC) > 0 were identified as DEGs. To identify ERRβ target genes, WT/Mock and KO/ERRβ-wt groups were compared with KO/Mock group to select DEGs. To classify the ERRβ target genes into classes 1–8, KO/Mock group was compared with groups of all combinations of each mutant expressing clones to obtain temporal DEGs. For example, the comparison of KO/Mock vs. KO/ERRβ-DBDm3 + KO/ERRβ-DBDm6 + KO/ERRβ-AF2M6 was used for class 8, and the comparison of KO/Mock vs. KO/ERRβ-DBDm3 + KO/ERRβ-AF2M6 was used for class 2. Then, if the temporal DEGs were found in the original ERRβ target genes, they were finally identified as the classified genes. If genes existed across multiple classes, those were allocated to one class according to the following priority: classes 1, 8 > 2, 3, 5 > 4, 6, 7. To identify ERRγ target genes, the ERRβ target genes were compared between KO/ERRγ and KO/ERRβ + WT/Mock groups, and DEGs were defined as non-ERRγ target genes.

Heatmaps were generated from z-score $\log_2$(transcripts per million) with complexHeatmap package. GO enrichment was computed by 'clusterProfiler's enrichGO' and compareCluster (v3.18.1).

To identify ERRβ binding region within ±50 kb from TSSs of the classified genes, the called peaks (q < 1E−5) of public ChIP-seq data performed with anti-ERRβ antibody and ESCs (SRX093166, SRX4004790, SRX4004792, SRX4158594, SRX4158595, SRX4167129, SRX4167130, SRX5023707, SRX5023708, SRX5023709, SRX5023710, ChIP-Atlas (https://chip-atlas.org)) were merged by Homer (v.4.10) to obtain ERRβ binding regions in ESCs (Supplementary information, Table S2). Next, the classified gene coordinates were obtained by 'TxDB.Mmusculus.UCSC.mm10.knownGene'. Then, ±50 kb window from each TSS was created by 'resize (gr, width = 100000, fix = "start")', and 'subsetByOverlaps' was run to select the regions that overlap the merged ERRβ binding regions and the ±50 kb windows. Then, we used Homer (v.4.10) for de novo motif enrichment analysis with 'findMotifGenome.pl -size 200 -mask' at the selected regions.

REFERENCES

1. Roeder, R. G. Role of general and gene-specific cofactors in the regulation of eukaryotic transcription. *Cold Spring Harb. Symp. Quant. Biol.* **63**, 201–218 (1998).
2. Allis, C. D. & Jenuwein, T. The molecular hallmarks of epigenetic control. *Nat. Rev. Genet.* **17**, 487–500 (2016).
3. Dancy, B. M. & Cole, P. A. Protein lysine acetylation by p300/CBP. *Chem. Rev.* **115**, 2419–2452 (2015).
4. Albright, S. R. & Tjian, R. TAFs revisited: more data reveal new twists and confirm old ideas. *Gene* **242**, 1–13 (2000).
5. Malik, S. & Roeder, R. G. The metazoan Mediator co-activator complex as an integrative hub for transcriptional regulation. *Nat. Rev. Genet.* **11**, 761–772 (2010).
6. Soutourina, J. Transcription regulation by the Mediator complex. *Nat. Rev. Mol. Cell Biol.* **19**, 262–274 (2018).
7. Roeder, R. G. The role of general initiation factors in transcription by RNA polymerase II. *Trends Biochem. Sci.* **21**, 327–335 (1996).
8. Orphanides, G., Lagrange, T. & Reinberg, D. The general transcription factors of RNA polymerase II. *Genes Dev.* **10**, 2657–2683 (1996).
9. Huss, J. M., Garbacz, W. G. & Xie, W. Constitutive activities of estrogen-related receptors: transcriptional regulation of metabolism by the ERR pathways in health and disease. *Biochim. Biophys. Acta* **1852**, 1912–1927 (2015).
10. Festuccia, N., Owens, N. & Navarro, P. Esrrb, an estrogen-related receptor involved in early development, pluripotency, and reprogramming. *FEBS Lett.* **592**, 852–877 (2018).
11. Giguere, V. Transcriptional control of energy homeostasis by the estrogen-related receptors. *Endocr. Rev.* **29**, 677–696 (2008).
12. Robyr, D., Wolffe, A. P. & Wahli, W. Nuclear hormone receptor coregulators in action: diversity for shared tasks. *Mol. Endocrinol.* **14**, 329–347 (2000).
13. Xu, J., Wu, R. C. & O'Malley, B. W. Normal and cancer-related functions of the p160 steroid receptor co-activator (SRC) family. *Nat. Rev. Cancer* **9**, 615–630 (2009).
14. Chen, W. & Roeder, R. G. Mediator-dependent nuclear receptor function. *Semin. Cell. Dev. Biol.* **22**, 749–758 (2011).
15. Wu, Z. et al. Mechanisms controlling mitochondrial biogenesis and respiration through the thermogenic coactivator PGC-1. *Cell* **98**, 115–124 (1999).
16. Puigserver, P. et al. Activation of PPARgamma coactivator-1 through transcription factor docking. *Science* **286**, 1368–1371 (1999).
17. Di, W. et al. PGC-1: The energetic regulator in cardiac metabolism. *Curr. Issues Mol. Biol.* **28**, 29–46 (2018).
18. Villena, J. A. & Kralli, A. ERRalpha: a metabolic function for the oldest orphan. *Trends Endocrinol. Metab.* **19**, 269–276 (2008).
19. Chen, W., Yang, Q. & Roeder, R. G. Dynamic interactions and cooperative functions of PGC-1alpha and MED1 in TRalpha-mediated activation of the brown-fat-specific UCP-1 gene. *Mol. Cell* **35**, 755–768 (2009).
20. Wallberg, A. E., Yamamura, S., Malik, S., Spiegelman, B. M. & Roeder, R. G. Coordination of p300-mediated chromatin remodeling and TRAP/mediator function through coactivator PGC-1alpha. *Mol. Cell* **12**, 1137–1149 (2003).
21. Malik, S. & Roeder, R. G. Isolation and functional characterization of the TRAP/Mediator complex. *Methods Enzymol.* **364**, 257–284 (2003).
22. Kim, J., Guermah, M. & Roeder, R. G. The human PAF1 complex acts in chromatin transcription elongation both independently and cooperatively with SII/TFIIS. *Cell* **140**, 491–503 (2010).
23. An, W. & Roeder, R. G. Reconstitution and transcriptional analysis of chromatin in vitro. *Methods Enzymol.* **377**, 460–474 (2004).
24. Sladek, R., Bader, J. A. & Giguere, V. The orphan nuclear receptor estrogen-related receptor alpha is a transcriptional regulator of the human medium-chain acyl coenzyme A dehydrogenase gene. *Mol. Cell. Biol.* **17**, 5400–5409 (1997).
25. Stein, R. A. et al. Estrogen-related receptor alpha is critical for the growth of estrogen receptor-negative breast cancer. *Cancer Res.* **68**, 8805–8812 (2008).
26. Schreiber, S. N. et al. The estrogen-related receptor alpha (ERRalpha) functions in PPARgamma coactivator 1alpha (PGC-1alpha)-induced mitochondrial biogenesis. *Proc. Natl. Acad. Sci. USA* **101**, 6472–6477 (2004).
27. Huss, J. M., Torra, I. P., Staels, B., Giguere, V. & Kelly, D. P. Estrogen-related receptor alpha directs peroxisome proliferator-activated receptor alpha signaling in the transcriptional control of energy metabolism in cardiac and skeletal muscle. *Mol. Cell. Biol.* **24**, 9079–9091 (2004).

28. Mootha, V. K. et al. Erralpha and Gabpa/b specify PGC-1alpha-dependent oxidative phosphorylation gene expression that is altered in diabetic muscle. *Proc. Natl. Acad. Sci. USA* **101**, 6570–6575 (2004).
29. Huss, J. M., Kopp, R. P. & Kelly, D. P. Peroxisome proliferator-activated receptor coactivator-1alpha (PGC-1alpha) coactivates the cardiac-enriched nuclear receptors estrogen-related receptor-alpha and -gamma. Identification of novel leucine-rich interaction motif within PGC-1alpha. *J. Biol. Chem.* **277**, 40265–40274 (2002).
30. Schreiber, S. N., Knutti, D., Brogli, K., Uhlmann, T. & Kralli, A. The transcriptional coactivator PGC-1 regulates the expression and activity of the orphan nuclear receptor estrogen-related receptor alpha (ERRalpha). *J. Biol. Chem.* **278**, 9013–9018 (2003).
31. Savkur, R. S. & Burris, T. P. The coactivator LXXLL nuclear receptor recognition motif. *J. Pept. Res.* **63**, 207–212 (2004).
32. Shao, G., Heyman, R. A. & Schulman, I. G. Three amino acids specify coactivator choice by retinoid X receptors. *Mol. Endocrinol.* **14**, 1198–1209 (2000).
33. Kallen, J. et al. Evidence for ligand-independent transcriptional activation of the human estrogen-related receptor alpha (ERRalpha): crystal structure of ERRalpha ligand binding domain in complex with peroxisome proliferator-activated receptor coactivator-1alpha. *J. Biol. Chem.* **279**, 49330–49337 (2004).
34. Bugge, A., Grontved, L., Aagaard, M. M., Borup, R. & Mandrup, S. The PPAR-gamma2 A/B-domain plays a gene-specific role in transactivation and cofactor recruitment. *Mol. Endocrinol.* **23**, 794–808 (2009).
35. Gelman, L. et al. p300 interacts with the N- and C-terminal part of PPARgamma2 in a ligand-independent and -dependent manner, respectively. *J. Biol. Chem.* **274**, 7681–7688 (1999).
36. Malik, S. et al. Structural and functional organization of TRAP220, the TRAP/mediator subunit that is targeted by nuclear receptors. *Mol. Cell. Biol.* **24**, 8244–8254 (2004).
37. Sonoda, J. et al. Nuclear receptor ERR alpha and coactivator PGC-1 beta are effectors of IFN-gamma-induced host defense. *Genes Dev.* **21**, 1909–1920 (2007).
38. Zhang, X. et al. MED1/TRAP220 exists predominantly in a TRAP/ Mediator subpopulation enriched in RNA polymerase II and is required for ER-mediated transcription. *Mol. Cell* **19**, 89–100 (2005).
39. Cevher, M. A. et al. Reconstitution of active human core Mediator complex reveals a critical role of the MED14 subunit. *Nat. Struct. Mol. Biol.* **21**, 1028–1034 (2014).
40. Malik, S., Baek, H. J., Wu, W. & Roeder, R. G. Structural and functional characterization of PC2 and RNA polymerase II-associated subpopulations of metazoan Mediator. *Mol. Cell. Biol.* **25**, 2117–2129 (2005).
41. Gearhart, M. D., Holmbeck, S. M., Evans, R. M., Dyson, H. J. & Wright, P. E. Monomeric complex of human orphan estrogen related receptor-2 with DNA: a pseudo-dimer interface mediates extended half-site recognition. *J. Mol. Biol.* **327**, 819–832 (2003).
42. Huppunen, J. & Aarnisalo, P. Dimerization modulates the activity of the orphan nuclear receptor ERRgamma. *Biochem. Biophys. Res. Commun.* **314**, 964–970 (2004).
43. Misawa, A. & Inoue, S. Estrogen-related receptors in breast cancer and prostate cancer. *Front. Endocrinol.* **6**, 83 (2015).
44. Sun, F. et al. Promoter-enhancer communication occurs primarily within insulated neighborhoods. *Mol. Cell* **73**, 250–263.e5 (2019).
45. Percharde, M. et al. Ncoa3 functions as an essential Esrrb coactivator to sustain embryonic stem cell self-renewal and reprogramming. *Genes Dev.* **26**, 2286–2298 (2012).
46. Yamane, M., Ohtsuka, S., Matsuura, K., Nakamura, A. & Niwa, H. Overlapping functions of Kruppel-like factor family members: targeting multiple transcription factors to maintain the naive pluripotency of mouse embryonic stem cells. *Development* **145**, dev162404 (2018).
47. Gaillard, S., Dwyer, M. A. & McDonnell, D. P. Definition of the molecular basis for estrogen receptor-related receptor-alpha-cofactor interactions. *Mol. Endocrinol.* **21**, 62–76 (2007).
48. Kamei, Y. et al. PPARgamma coactivator 1beta/ERR ligand 1 is an ERR protein ligand, whose expression induces a high-energy expenditure and antagonizes obesity. *Proc. Natl. Acad. Sci. USA* **100**, 12378–12383 (2003).
49. Monsalve, M. et al. Direct coupling of transcription and mRNA processing through the thermogenic coactivator PGC-1. *Mol. Cell* **6**, 307–316 (2000).
50. Luo, X. et al. Posttranslational regulation of PGC-1alpha and its implication in cancer metabolism. *Int. J. Cancer* **145**, 1475–1483 (2019).
51. Fernandez-Marcos, P. J. & Auwerx, J. Regulation of PGC-1alpha, a nodal regulator of mitochondrial biogenesis. *Am. J. Clin. Nutr.* **93**, 884S–890S (2011).
52. Ruas, J. L. et al. A PGC-1alpha isoform induced by resistance training regulates skeletal muscle hypertrophy. *Cell* **151**, 1319–1331 (2012).
53. Chymkowitch, P., Le May, N., Charneau, P., Compe, E. & Egly, J. M. The phosphorylation of the androgen receptor by TFIIH directs the ubiquitin/proteasome process. *EMBO J.* **30**, 468–479 (2011).
54. Traboulsi, H., Davoli, S., Catez, P., Egly, J. M. & Compe, E. Dynamic partnership between TFIIH, PGC-1alpha and SIRT1 is impaired in trichothiodystrophy. *PLoS Genet.* **10**, e1004732 (2014).
55. Compe, E. et al. Neurological defects in trichothiodystrophy reveal a coactivator function of TFIIH. *Nat. Neurosci.* **10**, 1414–1422 (2007).
56. Compe, E. et al. Dysregulation of the peroxisome proliferator-activated receptor target genes by XPD mutations. *Mol. Cell. Biol.* **25**, 6065–6076 (2005).
57. Holmbeck, S. M., Dyson, H. J. & Wright, P. E. DNA-induced conformational changes are the basis for cooperative dimerization by the DNA binding domain of the retinoid X receptor. *J. Mol. Biol.* **284**, 533–539 (1998).
58. Baumann, H. et al. Refined solution structure of the glucocorticoid receptor DNA-binding domain. *Biochemistry* **32**, 13463–13471 (1993).
59. Rimel, J. K. & Taatjes, D. J. The essential and multifunctional TFIIH complex. *Protein Sci.* **27**, 1018–1037 (2018).
60. Kolesnikova, O., Radu, L. & Poterszman, A. TFIIH: a multi-subunit complex at the cross-roads of transcription and DNA repair. *Adv. Protein Chem. Struct. Biol.* **115**, 21–67 (2019).
61. Fishburn, J., Tomko, E., Galburt, E. & Hahn, S. Double-stranded DNA translocase activity of transcription factor TFIIH and the mechanism of RNA polymerase II open complex formation. *Proc. Natl. Acad. Sci. USA* **112**, 3961–3966 (2015).
62. Kim, T. K., Ebright, R. H. & Reinberg, D. Mechanism of ATP-dependent promoter melting by transcription factor IIH. *Science* **288**, 1418–1422 (2000).
63. Fregoso, M. et al. DNA repair and transcriptional deficiencies caused by mutations in the Drosophila p52 subunit of TFIIH generate developmental defects and chromosome fragility. *Mol. Cell. Biol.* **27**, 3640–3650 (2007).
64. Malik, S., Molina, H. & Xue, Z. PIC activation through functional interplay between mediator and TFIIH. *J. Mol. Biol.* **429**, 48–63 (2017).
65. Osz, J. et al. Structural basis of natural promoter recognition by the retinoid X nuclear receptor. *Sci. Rep.* **5**, 8216 (2015).
66. Watson, L. C. et al. The glucocorticoid receptor dimer interface allosterically transmits sequence-specific DNA signals. *Nat. Struct. Mol. Biol.* **20**, 876–883 (2013).
67. Barry, J. B., Laganiere, J. & Giguere, V. A single nucleotide in an estrogen-related receptor alpha site can dictate mode of binding and peroxisome proliferator-activated receptor gamma coactivator 1alpha activation of target promoters. *Mol. Endocrinol.* **20**, 302–310 (2006).
68. Hutchins, A. P. et al. Co-motif discovery identifies an Esrrb-Sox2-DNA ternary complex as a mediator of transcriptional differences between mouse embryonic and epiblast stem cells. *Stem Cells* **31**, 269–281 (2013).
69. van den Berg, D. L. et al. Estrogen-related receptor beta interacts with Oct4 to positively regulate Nanog gene expression. *Mol. Cell. Biol.* **28**, 5986–5995 (2008).
70. Chen, X. et al. Integration of external signaling pathways with the core transcriptional network in embryonic stem cells. *Cell* **133**, 1106–1117 (2008).
71. Illingworth, R. S., Botting, C. H., Grimes, G. R., Bickmore, W. A. & Eskeland, R. PRC1 and PRC2 are not required for targeting of H2A.Z to developmental genes in embryonic stem cells. *PLoS One* **7**, e34848 (2012).
72. van den Berg, D. L. et al. An Oct4-centered protein interaction network in embryonic stem cells. *Cell Stem Cell* **6**, 369–381 (2010).
73. Albers, M. et al. Automated yeast two-hybrid screening for nuclear receptor-interacting proteins. *Mol. Cell. Proteomics* **4**, 205–213 (2005).
74. Dufour, C. R. et al. Genome-wide orchestration of cardiac functions by the orphan nuclear receptors ERRalpha and gamma. *Cell Metab.* **5**, 345–356 (2007).
75. Nakadai, T., Fukuda, A., Shimada, M., Nishimura, K. & Hisatake, K. The RNA binding complexes NF45-NF90 and NF45-NF110 associate dynamically with the c-fos gene and function as transcriptional coactivators. *J. Biol. Chem.* **290**, 26832–26845 (2015).
76. Fukuda, A. et al. Reconstitution of recombinant TFIIH that can mediate activator-dependent transcription. *Genes Cells* **6**, 707–719 (2001).
77. Luo, J. et al. A protocol for rapid generation of recombinant adenoviruses using the AdEasy system. *Nat. Protoc.* **2**, 1236–1247 (2007).
78. Yamaguchi, T. et al. Development of an all-in-one inducible lentiviral vector for gene specific analysis of reprogramming. *PLoS One* **7**, e41007 (2012).
79. Fukuda, A., Nogi, Y. & Hisatake, K. The regulatory role for the ERCC3 helicase of general transcription factor TFIIH during promoter escape in transcriptional activation. *Proc. Natl. Acad. Sci. USA* **99**, 1206–1211 (2002).
80. Okamoto, T. et al. Analysis of the role of TFIIE in transcriptional regulation through structure-function studies of the TFIIEbeta subunit. *J. Biol. Chem.* **273**, 19866–19876 (1998).
81. Tang, Z. et al. SET1 and p300 act synergistically, through coupled histone modifications, in transcriptional activation by p53. *Cell* **154**, 297–310 (2013).
82. Ito, M., Yuan, C. X., Okano, H. J., Darnell, R. B. & Roeder, R. G. Involvement of the TRAP220 component of the TRAP/SMCC coactivator complex in embryonic development and thyroid hormone action. *Mol. Cell* **5**, 683–693 (2000).

83. Kobayashi, T., Kato-Itoh, M. & Nakauchi, H. Targeted organ generation using Mixl1-inducible mouse pluripotent stem cells in blastocyst complementation. *Stem Cells Dev.* **24**, 182–189 (2015).
84. Niwa, H., Burdon, T., Chambers, I. & Smith, A. Self-renewal of pluripotent embryonic stem cells is mediated via activation of STAT3. *Genes Dev.* **12**, 2048–2060 (1998).
85. Ying, Q. L. et al. The ground state of embryonic stem cell self-renewal. *Nature* **453**, 519–523 (2008).
86. Guermah, M., Palhan, V. B., Tackett, A. J., Chait, B. T. & Roeder, R. G. Synergistic functions of SII and p300 in productive activator-dependent transcription of chromatin templates. *Cell* **125**, 275–286 (2006).
87. Shimada, M., Nakadai, T., Fukuda, A. & Hisatake, K. cAMP-response element-binding protein (CREB) controls MSK1-mediated phosphorylation of histone H3 at the c-fos promoter in vitro. *J. Biol. Chem.* **285**, 9390–9401 (2010).
88. Ogryzko, V. V. et al. Histone-like TAFs within the PCAF histone acetylase complex. *Cell* **94**, 35–44 (1998).
89. Shimada, M. et al. Gene-specific H1 eviction through a transcriptional activator–>p300–>NAP1–>H1 pathway. *Mol. Cell* **74**, 268–283.e5 (2019).
90. Poon, R. Y., Yamashita, K., Adamczewski, J. P., Hunt, T. & Shuttleworth, J. The cdc2-related protein p40MO15 is the catalytic subunit of a protein kinase that can activate p33cdk2 and p34cdc2. *EMBO J.* **12**, 3123–3132 (1993).
91. Kundu, T. K. et al. Activator-dependent transcription from chromatin in vitro involving targeted histone acetylation by p300. *Mol. Cell* **6**, 551–561 (2000).
92. Yu, M. et al. RNA polymerase II-associated factor 1 regulates the release and phosphorylation of paused RNA polymerase II. *Science* **350**, 1383–1386 (2015).
93. Cong, L. et al. Multiplex genome engineering using CRISPR/Cas systems. *Science* **339**, 819–823 (2013).
94. Cox, W. G. & Singer, V. L. A high-resolution, fluorescence-based method for localization of endogenous alkaline phosphatase activity. *J. Histochem. Cytochem.* **47**, 1443–1456 (1999).

ACKNOWLEDGEMENTS

This work was supported by NIH grants DK071900 and CACA234575 to R.G.R. T.N. was supported by JSPS KAKENHI (19K07651). M.S. was supported by JSPS KAKENHI (19K06482), K.I. by an NCI T32 grant (CA009673) and a JSPS fellowship for research abroad, and M.A.C. by an American Cancer Society Eastern Division — New York Cancer Research Fund Postdoctoral Fellowship. We thank Drs. Vincent Giguere for anti-ERRα antibody, Takashi Onikubo for a critical review of the manuscript, Masashi Yamaji for technical advice on CFA, Koji Hisatake for TFIIH expression constructs, and Roeder laboratory members for various assistance. We also acknowledge invaluable services from The Rockefeller University Flow Cytometry Resource Center (Svetlana Mazel, Director) and the Genomics Research Center (Connie Zhao, Director).

AUTHOR CONTRIBUTIONS

T.N. and R.G.R. planned the project. T.N. designed and conducted all experiments. M.S. provided the chromatin system. K.I. established ERRβ-KO ESCs and managed RNA-seq analysis. C.-S.C. and K.K. performed NGS data analyses. M.A.C. prepared anti-MED30 antibody and supported experiments with Mediator. R.M. supported ChIP experiments. T.N., S.M., and R.G.R. wrote the manuscript. All authors discussed the results and commented on the manuscript. R.G.R. supervised the overall work.

COMPETING INTERESTS

The authors declare no competing interests.

ADDITIONAL INFORMATION

Supplementary information The online version contains supplementary material available at https://doi.org/10.1038/s41422-022-00774-z.

Correspondence and requests for materials should be addressed to Robert G Roeder.

Reprints and permission information is available at http://www.nature.com/reprints